
Article:
Mulay, M.R., Patwardhan, S.V. orcid.org/0000-0002-4958-8840 and Martsinovich, N. orcid.org/0000-0001-9226-8175 (2024) Review of bio-inspired green synthesis of titanium dioxide for photocatalytic applications. Catalysts, 14 (11). 742. ISSN 2073-4344

https://doi.org/10.3390/catal14110742

---

catalysts

MDPI

Review

Review of Bio-Inspired Green Synthesis of Titanium Dioxide for Photocatalytic Applications

Manasi R. Mulay [1,2,†], Siddharth V. Patwardhan [3] and Natalia Martsinovich [1,*]

[1] Department of Chemistry, University of Sheffield, Sheffield S3 7HF, UK
[2] Grantham Centre for Sustainable Futures, University of Sheffield, Sheffield S3 7RD, UK
[3] Department of Chemical and Biological Engineering, University of Sheffield, Sheffield S1 3JD, UK; s.patwardhan@sheffield.ac.uk
* Correspondence: n.martsinovich@sheffield.ac.uk
† Current address: School of Minerals, Metallurgical and Materials Engineering, Indian Institute of Technology, Bhubaneswar 752050, India.

Abstract: Titanium dioxide (TiO_2) is an important photocatalyst that is widely studied for environmental applications, especially for water treatment by degradation of pollutants. A range of methods have been developed to produce TiO_2 in the form of nanoparticles and thin films. Solution-based synthesis methods offer the opportunity to tune the synthesis through a choice of reagents, additives and reaction media. In particular, the use of biomolecules, such as proteins and amino acids, as bio-inspired additives in TiO_2 synthesis has grown over the last decade. This review provides a discussion of the key factors in the solution-based synthesis of titania, with a focus on bio-inspired additives and their interaction with Ti precursors. In particular, the role of bio-inspired molecular and biomolecular additives in promoting the low-temperature synthesis of titania and controlling the phase and morphology of the synthesised TiO_2 is discussed, with a particular focus on the interaction of TiO_2 with amino acids as model bio-inspired additives. Understanding these interactions will help address the key challenges of obtaining the crystalline TiO_2 phase at low temperatures, with fast kinetics and under mild reaction conditions. We review examples of photocatalytic applications of TiO_2 synthesised using bio-inspired methods and discuss the ways in which bio-inspired additives enhance photocatalytic activity of TiO_2 nanomaterials. Finally, we give a perspective of the current challenges in green synthesis of TiO_2, and possible solutions based on multi-criteria discovery, design and manufacturing framework.

Keywords: TiO_2; bio-inspired; green synthesis; amino acids; sustainable; photocatalyst

Citation: Mulay, M.R.; Patwardhan, S.V.; Martsinovich, N. Review of Bio-Inspired Green Synthesis of Titanium Dioxide for Photocatalytic Applications. *Catalysts* **2024**, *14*, 742. https://doi.org/10.3390/catal14110742

Academic Editor: Fei Chang

Received: 22 August 2024
Revised: 15 October 2024
Accepted: 17 October 2024
Published: 22 October 2024

1. Introduction

Photocatalysis plays a key role in the pursuit to replace fossil fuels with renewable resources, such as sunlight, by harvesting energy from light to drive a variety of industrially and environmentally important processes, such as the degradation of pollutants in air and water, hydrogen production from water splitting, CO_2 reduction and organic synthesis [1–5]. In particular, photocatalysis has emerged as an effective technique to destroy pollutants via photoinduced oxidation processes [5,6]. In photocatalytic water treatment, photocatalyst materials absorb light to form photogenerated electrons and holes, which then react with water molecules to produce reactive oxygen species, such as hydroxyl radicals, which are able to oxidise organic pollutants to small non-toxic fragments. Photocatalytic water treatment complements conventional water treatment techniques, which have limitations and are unable to completely eliminate harmful pollutants from water [6,7]. However, advanced water treatment methods themselves have environmental impacts, such as high energy use, infrastructure costs [8–10] and the large amount of energy required for the synthesis of photocatalyst materials [9,11,12]. Hence, it is important to minimise the environmental impact of advanced oxidation processes (AOPs), e.g., by using renewable

energy in water treatment processes [10]. In particular, the problem of the energy-intensive synthesis of photocatalysts can be solved by developing methods for the green synthesis of photocatalysts [12].

Titanium dioxide is the most widely used photocatalyst [13,14]. Since 1972, when Honda and Fujishima first investigated the photocatalytic properties of TiO_2, titanium dioxide has been a popular choice as a photocatalyst material, due to its photocatalytic efficiency, photostability when being reused, cost effectiveness and environmental sustainability [13,15–17]. TiO_2 can exist in three polymorphs: anatase, rutile and brookite. Rutile is thermodynamically more stable, but anatase and brookite display a higher photocatalytic efficiency [18–20]. Furthermore, the metastable monoclinic bronze phase of TiO_2 was found to have high photocatalytic activity [21]. Photocatalytic efficiency also depends on the exposed crystal facets, and the less stable (001) facet of anatase is photocatalytically more active than the more stable (101) facet [22].

The photocatalytic degradation of organic pollutants in water using TiO_2 photocatalysts is restricted by the limitations of this material, such as its large bandgap, light scattering due to the small particle size, and reduction in the number of active sites due to the agglomeration of particles [23]. To address these limitations, controlled synthesis strategies are needed to tailor the crystal structure and morphology and to broaden the photoresponse of TiO_2 using surface functionalisation.

Titanium dioxide photocatalysts are utilised in suspension, as thin films or coatings or as powders in catalytic beds. The synthesis of the powder or particle form of titanium dioxide photocatalysts can be generally carried out by solution-based synthesis [24] or solid-state methods [25], whereas thin-film deposition and coatings can be achieved by gas-phase synthesis [26]. Gas-phase or vapour-phase thin-film coating and deposition techniques include thermal evaporation [27], thermal plasma technology [28], sputtering [29,30] and chemical vapour deposition (CVD) [31–33]. However, gas-phase synthesis can also produce the powder form of TiO_2, while the powder obtained from liquid-phase synthesis can be blade-coated to make thin films.

Solution-based synthesis methods promise better control over morphology compared to solid-phase and gas-phase synthesis methods. The solution synthesis route includes methods such as sol-gel, solvothermal, hydrothermal and precipitation syntheses [24,34]. These methods produce crystalline titanium dioxide after post-synthetic heat treatment.

Using solution-based techniques, the structural and functional properties of nanocrystalline particles or coatings can be controlled by selecting the synthesis parameters, which are summarised in Figure 1. The key parameters in the solution synthesis are precursors, chemical reagents and conditions. The selection of reagents for synthesis includes the type of precursor, type of additive, type of solvent, the precursor to additive ratio and the pH of the solution. Additional factors are the reaction temperature, calcination temperature, reaction time and aging time.

The conventional techniques of solution-based or liquid-phase synthesis require high-precision equipment [28], a high energy input, toxic chemical additives and capping or chelating agents [34] and involve high processing costs [35]. Since the principles of sustainable and green chemistry aim to minimise the energy, cost and environmental impacts of synthesis processes, low-temperature synthesis methods are desirable for green synthesis [36].

The least energy-intensive choices for solution synthesis would be the preferred route for the sustainable synthesis of TiO_2, maintaining the product quality without increasing the resource intensity. Ideally, a technique is needed to synthesize crystalline titanium dioxide at room temperature. One possible route to achieve this is through the use of biomolecules or bio-inspired additives [37].

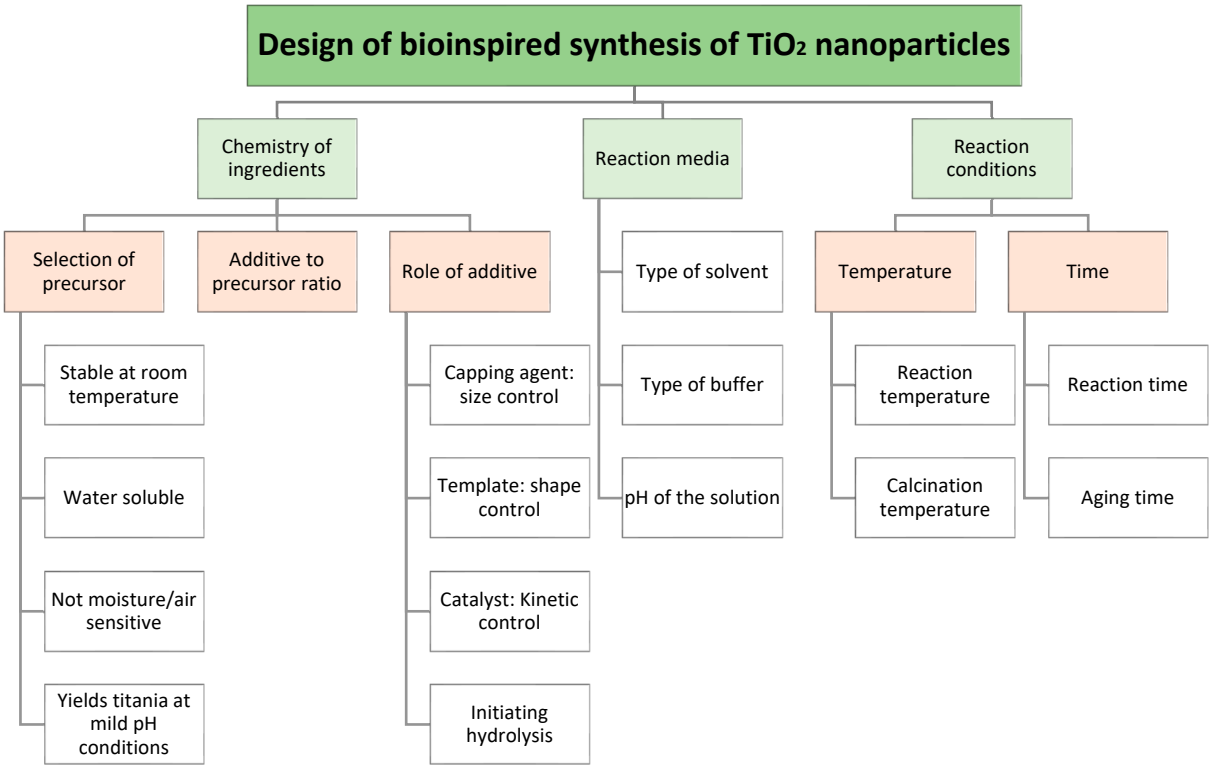

Figure 1. Design parameters for titanium dioxide synthesis via solution chemistry route.

Bio-mineralisation processes have been occurring in nature for millennia and involve the assistance of biomolecules in the formation of inorganic materials in living organisms [38,39]. In the past two decades, various biomolecules associated with biological and non-biological minerals have been identified and employed successfully for the in vitro synthesis and growth of inorganic nanostructures of metals, oxides and semiconductors [37,40,41]. Biomolecules, such as amino acids, peptides and proteins, have a critical role in mineralisation due to the specificity of their interactions with minerals, and they can also act as templates to produce nanostructures [37,40–43]. There are two ways to tap into the potential of biomineralization in material synthesis: (i) the direct use of biomolecules that exist in nature; and (ii) developing molecules in the lab that mimic or are inspired by natural biomolecules [44].

Besides the challenges associated with synthesis processes, the scale and sustainability associated with the synthesised materials also need to be considered. By addressing multiple goals at the same time, through the approach of 'multicriteria thinking', the full potential of bio-inspired additives for nanomaterials synthesis can be tapped [45].

The focus of this review is exploring the role of bio-inspired molecular additives in the synthesis of TiO_2. Specifically, this review provides a comprehensive and critical analysis of the effects of molecular additives and links them to chemical interactions underlying the reactions of TiO_2 formation. While there have been several recent reviews on TiO_2 synthesis using nature-based additives, such as plants [46–49], there is a lack of reviews focussed on the role of molecular and biomolecular additives, such as short peptides, amino acids and other "simple" molecules. The reviews of plant-based additives have largely focussed on synthesis procedures and precursors and on applications of TiO_2 products, rather than on mechanisms and interactions responsible for TiO_2 formation. The focus on "simple" additives in this review will help identify key future directions, e.g., investigating TiO_2–additive chemical interactions, which ultimately can lead to TiO_2 synthesis in a controllable manner instead of trial and error.

This review discusses the use of bio-inspired additives for synthesising titanium dioxide by considering multiple reaction design parameters. The key factors affecting

the synthesis of titanium dioxide (Figure 1) are discussed, with a particular focus on the bio-inspired synthesis of TiO_2. The aim is to provide an overview of the state-of-the-art solution synthesis methods for titanium dioxide, including various bio-inspired methods, and to discuss their merits and limitations to serve as a platform for further research in this area. Finally, as a key application, the photocatalytic performance of TiO_2 synthesized by green synthesis methods is reviewed.

2. Choice of Synthesis Parameters

2.1. Selection of Precursor

Titanium (IV) compounds, such as titanium tetrachloride ($TiCl_4$), titanium alkoxides and titanium bis (ammonium lactate) dihydroxide (TiBALDH), are the most commonly used precursors for the synthesis of titanium dioxide via solution synthesis. Titanium tetrachloride ($TiCl_4$) reacts with water exothermically to form titanium dioxide and HCl. Table S1 (Supplementary Materials) presents several examples of TiO_2 synthesis using a $TiCl_4$ precursor. However, one of the downsides of using $TiCl_4$ is the formation of orthotitanic acid (H_4TiO_4) as a byproduct. As the formation of orthotitanic acid cannot be avoided, it may hamper the homogeneity of the titanium dioxide synthesised using $TiCl_4$ [50]. The $TiCl_4$ precursor is also volatile and can react with atmospheric moisture and thus requires a fume cupboard during its use [51].

An alternative precursor, TiF_4, is more stable than $TiCl_4$ and can be used for the selective formation of {001} facets of anatase, which are highly reactive and therefore beneficial for applications such as photocatalysis [52]. For example, a mixture of $TiCl_4$ and TiF_4 precursors were used to achieve the controlled synthesis of {101} and {001} facets [53]. Although TiF_4 is good for facet-specific synthesis [22], its dissociation to form extremely harmful HF at higher temperatures makes TiF_4 a less desirable choice.

Titanium (IV) alkoxides are another type of commonly used precursors for sol-gel synthesis of titanium dioxide, which go through hydrolysis and a condensation reaction to form TiO_2. Table S2 lists examples of studies that have used Ti isopropoxide and Ti butoxide precursors. Due to their poor solubility, alkoxides hydrolyse slowly. Their rate of hydrolysis can be controlled by the pH and the type of catalyst used (e.g., hard vs. soft acid) [54]. However, due to the electronegativity of alkoxy groups, titanium alkoxides are very sensitive to nucleophilic attack by water [55] and can be hydrolysed even by reacting with moisture in the atmosphere. Precursors that are less sensitive to environmental conditions, such as moisture in the air, are required in order to avoid early hydrolysis, which could hinder the degree of control over the synthesis [34].

In order to avoid the use of non-aqueous solvents, an ideal precursor needs to be water soluble. Ti (IV) sulfates, glycolates and lactates are examples of water-soluble precursors. For example, titanium sulfate $Ti(SO_4)_2$ precursors were used for TiO_2 synthesis by solvothermal or hydrothermal methods [56–59]. Ti oxysulfate was used as a precursor and exhibited a co-operative effect in the amino acid lysine-assisted synthesis of TiO_2, to yield single crystals of anatase TiO_2 with exposed {101} and {100} facets [60].

Titanium (IV) bis (ammonium lactato) dihydroxide (TiBALDH), also known as TALH or ALT, is a water-soluble titanium precursor which is stable at neutral pH conditions at room temperature [37,61–63]. TiBALDH does not hydrolyse under ambient conditions, but it was found that an aqueous solution of urea can slowly hydrolyse it at 90 °C [64]. The hydrolysis of TiBALDH at a high pH was reported to be better controlled compared to the hydrolysis of Ti alkoxides, with aqueous NaOH decomposing TiBALDH to TiO_2, NH_3 and sodium lactate [61]. The conversion of TiBALDH to TiO_2 was found to occur due to a coordination equilibrium, as shown in Equation (1), where TiBALDH in the form of ammonium oxo-lactato-titanate $(NH4)_8Ti_4O_4(Lactate)_8$ in solution is in equilibrium with ammonium tris-lactato-titanate, $(NH_4)_2Ti(Lactate)_3$ (with its structure shown in Figure 2)

and TiO_2, so that uniform crystalline TiO_2 anatase nanoparticles are formed even at room temperature and are stabilized by surface-capping lactate ligands [62].

$$3\ [Ti_4O_4(Lactate)_8]^{8-} + 8\ NH_4^+ \rightleftharpoons 8\ [Ti(Lactate)_3]^{2-} + 4\ TiO_2 + 8\ NH_3 + 4\ H_2O \quad (1)$$

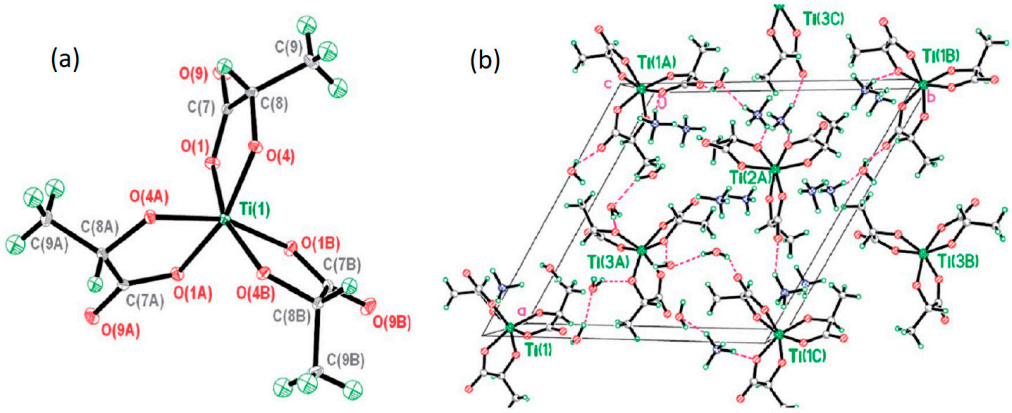

Figure 2. (**a**) Molecular structure of $[Ti(Lactate)_3]^2$; (**b**) unit cell of $(NH_4)_2[Ti(L\text{-}Lactate)_3]\cdot 3H_2O$ based on X-ray crystal diffraction results (reproduced with permission from Ref. [62]).

In summary, the TiBALDH precursor stands out as an ideal precursor for bio-inspired synthesis of titania based on the criteria listed in Figure 1, and it has become a popular precursor choice for bio-inspired synthesis, used in multiple studies as shown in Table 1.

Besides these main types of Ti precursors, other precursors have been used: for example, $TiCl_3$ was used to produce the rutile [65] and anatase phases of TiO_2 [65,66], as well as the "bronze" phase of TiO_2 [21]. The rutile, brookite and bronze phases of TiO_2 were also obtained using Ti metal powder dissolved in hydrogen peroxide [21,67,68].

Table 1. Titanium dioxide synthesis using TiBALDH precursor.

Solvent	Additives	Reaction Temperature	Reaction Time	Calcination Temperature	Product	Ref.
Deionized water	Urea	RT, then 100 °C	1 h at RT, 20 h at 100 °C	500 °C	Amorphous thin-film coating	[64]
Aqueous solution	Urea	160 °C	Overnight	300–550 °C	Pure anatase, pure brookite or biphasic anatase/brookite mixtures	[69]
Water	Urea	95 °C	24 h	-	Anatase TiO_2 sol	[70]
Water	L-arginine	RT	30 min	480 °C	Anatase	[71]
Tris–HCl buffer	Arginine	RT	0.5–10.0 min	-	Anatase	[72]
Water, phosphate buffer	Spermidine or spermine	RT	Overnight	200, 400, 600, 800 °C	Anatase after annealing at 800 °C	[73]
Aqueous solution	Poly(allylamine hydrochloride), poly(diallyldimethyl-ammonium chloride)	RT	5–60 days	-	Aggregated nanoparticles of anatase (anatase was observed after 30 days)	[74]
Phosphate-citrate buffer solution	c-terminal tetra peptide Gly-Gly-Gly-Trp	RT	10 min	-	Nanoparticles <50 nm in size contained very fine (<10 nm) anatase and monoclinic TiO_2 domains	[75]
Tris buffer	Serine-lysine (S-K) peptides KSSKK, $SKSK_3SKS$	RT	24 h	-	Amorphous or crystalline particles, 150–1200 nm diameter	[76]

Table 1. *Cont.*

Solvent	Additives	Reaction Temperature	Reaction Time	Calcination Temperature	Product	Ref.
Water	KIIIIKYWYAF peptide	70 °C	48 h	580 °C	Anatase after 580 °C	[77]
Phosphate buffer or water	R5 peptide or poly-L-lysine-hydrobromide	RT	5 min	600–900 °C	Anatase at 600 °C. Anatase to rutile transition was at 700 °C	[78]
Tris or phosphate buffer	R5 peptide and its truncated analogues	RT	24 h	600 °C	Amorphous TiO_2 at RT; anatase formed after annealing at 600 °C	[79]
Tris buffer, phosphate buffer or distilled water	Titanium dioxide binding peptides Ti-1, Ti-2 and R5	RT	2–72 h	-	<10 nm TiO_2 sols, mostly amorphous with some anatase and monoclinic phases	[41]
Phosphate buffer	R5 peptide	RT		-	TiO_2 nanosheets several µm in size, amorphous with <10 nm anatase domains	[80]
Citrate buffer	Car9 peptide fused to superfolder green fluorescent protein (sfGFP)	RT	120 min	-	Mixture of amorphous, anatase and monoclinic (bronze) TiO_2 phases	[81]
Deionized water	Silicatein protein	20 °C	24 h (at 20 °C), 1 h (calcination)	27–927 °C in steps of 100 °C	Mixture of amorphous and nanocrystalline anatase; transition to rutile was at 850 °C	[37]
Tris-HCl buffer	Proteins protamine, lysozyme, gelatin, haemoglobin, yeast alcohol dehydrogenase and bovine serum albumin	RT	5 min	600–700 °C	Amorphous at RT; transition to anatase at 600–700 °C and to rutile at 800 °C	[82]
Phosphate-buffered saline (PBS)	Bioengineered silicatein α and β and scaffold protein silintaphin-1	RT	12 h	-	Amorphous and anatase phases	[83]
Water, phosphate/ citrate buffer	Silaffin protein	RT	20 min	-	Rutile	[40]

2.2. Role of Solvent, pH and Buffer

The choice of solvent affects the equilibrium between the TiBALDH precursor and TiO_2, as described in Equation (1). This equilibrium can be shifted towards TiO_2 by using a less polar solvent, such as methanol or ethanol, diluting the solution, introducing salts or raising the temperature. In contrast, the use of polar and strongly solvating media, such as dimethyl sulfoxide, shifts the equilibrium towards reactants [62]. The ability to reverse the direction of the reaction is essential for producing nanocrystalline and monodisperse TiO_2 at room temperature. This is because once TiO_2 crystallites have nucleated, if the reaction is able to proceed backwards towards the reactants, then it restricts further agglomeration, leading to a smaller particle size.

It is well established that anatase formation is preferred to rutile at higher (basic) pH levels in aqueous media, whereas rutile is more prone to forming in acidic media [84]. This is explained by the mechanism of condensation of precursor $[Ti(OH)_x(H_2O)_y]^{n+}$ complexes: at high pH levels, the Ti complexes contain more OH groups, resulting in the edge sharing of octahedra, leading to the anatase phase. In contrast, at lower pH levels with few OH ligands, rutile formation takes place due to the corner bonding of the octahedra [84,85]. The conversion between TiO_2 phases can be achieved by controlling the pH of the solution: for example, amorphous anatase was reported as the initial product of the hydrolysis of the titanium isopropoxide precursor, which was converted to anatase and then to rutile upon the

addition of acid [86]. It was hypothesized that the anatase-to-rutile conversion was accelerated in the acidic medium thanks to the formation of an intermediate metastable ionic phase $[Ti(OH)_2]^{2+}$, which lowered the energy barrier for the anatase-to-rutile transformation [86].

The pH of a solution can be controlled by adding a buffer solution. For example, phosphate, citrate or tris(hydroxymethyl)aminomethane (Tris) HCl buffers are commonly used. The influence of pH on TiO_2 synthesis was investigated using buffers with the TiBALDH precursor [63] in bio-inspired syntheses using different biomolecule additives, such as peptides [76,78], polyamines [73] and amino acids [87]. Complex trends were observed, depending both on the pH and on the nature of the biomolecule additives. For example, a study of TiO_2 formation using a peptide additive with phosphate buffers ranging between pH levels of 5.5 to 7.5 found that the TiO_2 production rate reached the maximum in the pH range of 6.0–7.5, and a pH of 7.5 yielded well-defined particles [78]. A study of TiO_2 formation using polyamine additives showed different pH dependence trends depending on the length of the polyamine chain: long-chain polyamine spermine enabled TiO_2 formation in a wide range of pH levels between 2.9 and 12.6, while a medium-chain polyamine spermidine enabled TiO_2 formation only at acidic and neutral pH levels, up to a pH of 9.5, as depicted in the scanning electron microscopy (SEM) images in Figure 3 [73].

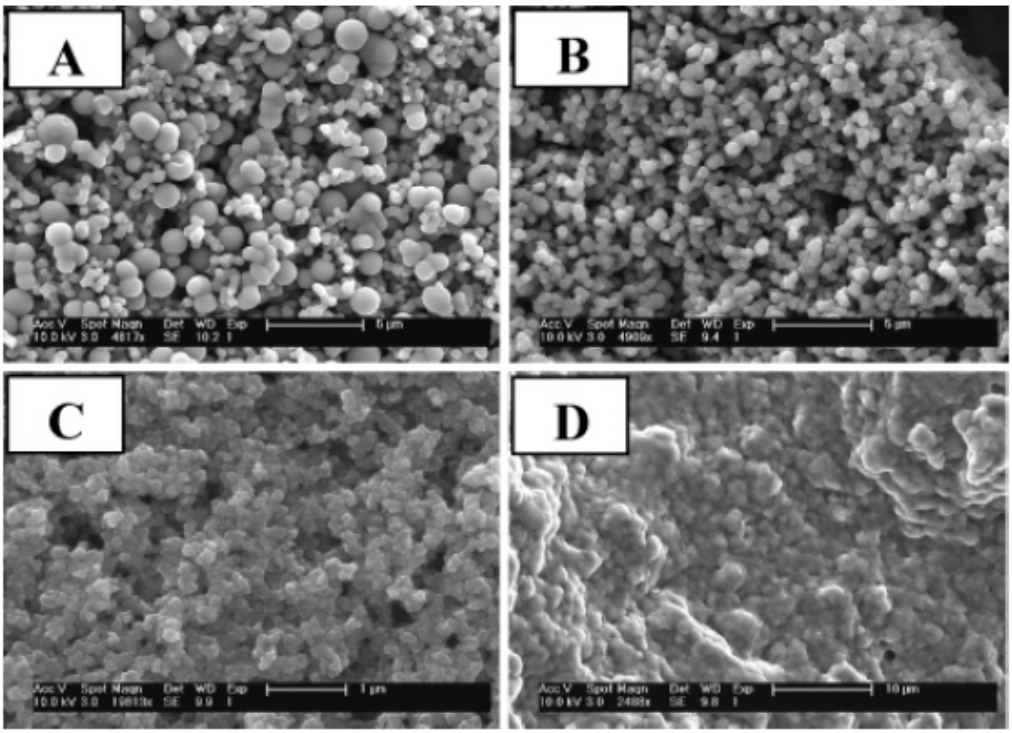

Figure 3. SEM images of the products of spermidine-assisted TiO_2 synthesis at (**A**) pH of 6.7, (**B**) pH of 8.9, (**C**) pH of 9.3 and (**D**) pH of 9.9. TiO_2 polyhedra are seen at pH of 6.7–8.9, while decrease in structure is seen above pH of 9, and unstructured solid is seen at pH of 9.9 (reproduced with permission from Ref. [73]).

Furthermore, the effect of pH on the crystalline phase of the final TiO_2 product was investigated in depth in amino-acid-assisted synthesis [87]. Syntheses using a series of amino acids produced anatase as the dominant phase at pH levels of 1 to 6, while only amorphous titania was formed at a pH of 8. However, in addition to the anatase phase, a secondary TiO_2 crystalline phase was obtained in some cases, with the amount and nature of this secondary phase dependent both on the pH and on the nature of the amino acid additives. For example, glycine, lysine and arginine produced a mixture of anatase and rutile at a pH of 1 and a mixture of anatase and brookite with pH levels from 2 to 6 [87]. This is consistent with the previously reported preference for the rutile phase at an acidic

pH and the anatase phase at a more basic pH [84–86]. In contrast, aspartic acid, glutamic acid and serine produced only the anatase phase in the range of pH levels from 1 to 6, while histidine and proline produced a mixture of anatase and brookite with pH levels from 1 to 4 and pure anatase at a pH of 6. This study revealed a complex interplay of the effects of pH levels and amino acid additives, which are analysed in more detail in Section 3.1, in which the effects of additives are discussed.

Beyond investigating the effect of the pH, the effect of the chemical nature of the buffer on the mechanism of peptide-assisted TiO_2 mineralisation was investigated by synthesizing TiO_2 sol particles at a pH of 7.4 maintained in NaOH solution, Tris buffer and phosphate buffer [41]. Tris buffer and non-buffered aqueous solutions produced monodisperse crystalline TiO_2 particles, while the phosphate buffer solution produced polydisperse, poorly crystalline particles with the presence of some adsorbed phosphate. This co-precipitation of TiO_2 with phosphate indicated that the nature of the buffer can affect the TiO_2 condensation reaction and in particular showed that titanium phosphates are formed instead of pure TiO_2 in Ti–polymer complexation, thus disrupting TiO_2 crystallisation [41].

3. Bio-Inspired Additives

Research on bio-inspired additives for titanium dioxide synthesis has emerged over the last two decades. A wide range of biomolecules, such as amines, amino acids, peptides and proteins, as well as organic matter and organic waste, have been employed as additives for the synthesis of TiO_2 nanomaterials. Biomaterials originating directly from nature have also been explored for the synthesis of TiO_2, including plant derivatives such as pomelo peel [88], jatropha leaves [89], pollen grains [90], green tea extract, aloe vera gel [91], leaf extracts of morinda citrofolia [92], parthenium hysterophorus [93] and eucalyptus globulus [94] as nature-based additives. Besides the plant-based extracts, microbes such as fungi and bacteria have been used for TiO_2 synthesis [46–48,95]. Recent reviews on the bio-inspired synthesis of TiO_2 list various plant-based and microbe-based TiO_2 synthesis studies [46–49]. However, the direct use of biomolecules from nature has limitations in terms of up-scaling due to their availability. Thus, a trend of using synthetic analogues of natural biomolecules is emerging. These bio-inspired additives have been employed for the synthesis of nanomaterials [39,44].

The use of biomolecules as additives for TiO_2 synthesis was pioneered by Morse et al., who synthesised TiO_2 using silicatein, a protein derived from marine silica sponges, as a template [37]. Further TiO_2 nanoparticle synthesis studies have used a variety of proteins [40,81–83,96] and peptides [41,43,75–78], as well as enzymes such as protease and lipase [97]. Following on from peptides and proteins, biomolecular additives with simpler chemical structures were used, such as amines and polyamines [74,98,99] and amino acids [60,87,100–103].

For example, Cole and Valentine investigated several naturally occurring polyamines as additives for TiO_2 synthesis and found that the chemical nature of the polyamines was a significant factor: the polyamines spermine and spermidine reacted with Ti precursors to form TiO_2, while the shorter diamines putrescine and cadaverine did not result in TiO_2 mineralisation [73]. They concluded that the number of amine functionalities in the polyamines played a significant role in the titanium mineralisation: while diamines could bind to a single Ti atom by bidentate chelation, polyamines such as spermine and spermidine with three or more amine groups could bind to multiple Ti atoms and induce condensation to form TiO_2.

Amino acids, as the simplest building blocks of proteins, have been widely used for the bio-inspired synthesis of TiO_2 (Table 2) [60,100–103]. The use of amino acids enables the testing of the effect of variables, such as the charge of the biomolecule and its degree of protonation at a particular pH. Amino-acid-assisted synthesis was found to produce various phases of TiO_2 nanoparticles both after annealing [71,100,102–104] and in room-temperature synthesis [60,72,87]. For example, the synthesis of TiO_2 from $TiCl_4$ precursors using a series of amino acids as additives at a range of pH levels resulted in mixtures of

anatase, rutile and brookite [87]. Another study using TiBALDH as a precursor and arginine as an additive produced anatase particles, with 3,4-dihydroxy-L-phenylalanine (dopa) then added to terminate the reaction and to control the size of the synthesized nanoparticles between 35 and 350 nm [72]. Solvothermal synthesis at 160 °C using titanium oxysulfate as a precursor and lysine as an additive in an acidic medium provided anatase single crystals with facet control [60]. Beyond TiO_2, amino acids have also been employed in the synthesis of various metal oxides, such as ZnO [105], WO_3 [106], SnO_2 [107], perovskite nanoparticles [108] and metal nanoparticles, such as Ag [109], Pd nanocrystals [110] and bimetallic PtCo nanospheres [111]. Besides synthesis, mechanistic studies of the bio-assisted synthesis of TiO_2 have been carried out. These mechanistic aspects are discussed below, with a particular focus on the role of bio-inspired additives as catalysts and templates.

Table 2. Amino-acid-assisted titanium dioxide synthesis.

Ti Precursor	Types of Amino Acids	Process	Calcination	TiO_2 Phase	TiO_2 Morphology	Ref.
Titanium n-butoxide ($Ti(OBu)_4$	Glycine	Hydrothermal synthesis at 120 °C for 48 h	500 °C; 3.5 h	Anatase	Flower-like hierarchical spheres with a 2 µm diameter assembled on 20 nm thick nanosheet	[102]
Titanium isopropoxide	Glycine, $_{DL}$-alanine, β-alanine, $_{DL}$-valine, proline, serine, $_{DL}$-aspartic acid, $_{L}$-glutamic acid	Gel formation after 12 h at room temperature, drying at 100 °C	500 °C; 3 h	Anatase	10–15 nm cubic particles	[101]
TiBALDH	Arginine	g-C_3N_4 + distilled water; 30 min at room temperature	480 °C; 2 h	Anatase	Uniformly distributed TiO_2 nanoparticles, d < 10 nm on g-C_3N_4 nanosheets	[71]
Titanium n-butoxide ($Ti(OBu)_4$	Glycine	200 °C for 20 h	450 °C; 5 h	Anatase	Hollow microspheres, with a crystallite size of 4.8 nm	[103]
$TiCl_4$	Glycine, alanine, serine, threonine, β-alanine	Seeded growth of TiO_2 nanorods in HCl on pre-annealed FTO glass. Seeds grown at 95 °C	450 °C; 1 h	Rutile	300–900 nm nanorods on FTO glass	[100]
Titanium isopropoxide (TTIP)	L-alanine	TTIP, L-alanine and dodecylamine in ethyl alcohol reacted at 60 °C for 24 h	400 °C; 4 h	Anatase	200 nm nanoparticles	[112]
Titanium isobutoxide	L-lysine	60 °C 20 h; 100 °C 24 h	350 °C	Mixed phase anatase + brookite	Mesoporous nanocrystals	[113]
Titanium (IV) oxysulfate	Lysine	Solvothermal synthesis in precursor in diluted H_2SO_4 at 160 °C 24 h	No further calcination	Anatase with exposed {101} and {111} facets	Single-crystal-like hierarchical spheres	[60]

Table 2. *Cont.*

Ti Precursor	Types of Amino Acids	Process	Calcination	TiO_2 Phase	TiO_2 Morphology	Ref.
$TiCl_4$	Glycine, glutamic acid, aspartic acid, serine, histidine, proline, lysine, arginine	Thermo-hydrolysis at 60 °C, from 1 day to 1 week, at a pH of 1 to 8	No further calcination, but long reaction time	Anatase, brookite, anatase + brookite, anatase + rutile, amorphous	Nanoparticles with controlled shapes and sizes	[87]
TiBALDH	Arginine, serine, lysine, histidine, glycine	10 min at room temperature	No further calcination	Surface functionalised anatase only with arginine	35–350 nm nanoparticles	[72]

3.1. Influence of Bio-Inspired Additives on Reaction Kinetics and Phase Control

Several studies have demonstrated the role of amino acid, peptide and protein additives as catalysts, which influence reaction kinetics by lowering the time and/or the temperature required for the TiO_2 synthesis reaction [72,74–76,81,87,100,114]. For example, in the glycine-assisted synthesis of TiO_2 nanorods, the rate of hydrolysis of the titanium tetrachloride precursor was found to depend on the amino acid concentration: an increase in the concentration of glycine increased the rate of the reaction, confirming the catalyst-like behaviour of glycine in synthesizing TiO_2 nanoparticles [100]. In another example of catalytic action of amino acid additives, arginine was found to act as a catalyst for TiO_2 nanoparticle nucleation and growth, with the size of synthesized TiO_2 nanoparticles increasing both with time and with the increased concentration of arginine [72]. These examples from the literature suggest that amino acids act as catalysts by lowering the temperature of crystalline-phase formation, while the reaction time in these studies varies between several days and several minutes depending on the additive and processing conditions (Table 2) [72,87].

Besides the initial precursor hydrolysis, the use of bio-inspired additives affects the next step of synthesis—calcination. As seen in Tables 1 and 2 and in Tables S1 and S2 in the Supplementary Materials, the conventional synthesis procedure generally involves two steps, in which the first step is the precursor's hydrolysis, and the second step is calcination at a high temperature, which is required to obtain crystalline TiO_2.

It can be seen from the compilation of studies from the literature in Table 1 that amorphous TiO_2 is commonly formed from various Ti precursors at room temperature, while post-synthesis heat treatment at 700 °C or 800 °C is required to produce the crystalline anatase or rutile phase, respectively. However, as seen in Tables 1 and 2, biomolecule-assisted syntheses can produce crystalline TiO_2 at low temperatures below 100 °C [40,72,74,75,83,87,100]. In particular, some amino acids, amines, peptides and protein additives can promote the synthesis of crystalline TiO_2 at room temperature without calcination [41,72,74–76,81,87].

The calculation temperatures required for anatase and rutile phase formation are highly additive-dependent: for example, syntheses using silicatein and protamine protein additives required higher temperatures for the anatase-to-rutile transformation compared to the alkali-catalysed hydrolysis of TiO_2 precursors without additives [37,82]; this was attributed to intermediate formation of composites between the Ti precursors and proteins, which may have prevented the crystallisation of amorphous titania, and to the strain imposed by the proteins on the crystal surfaces [37,82]. While silicatein was the protein of choice in the early studies because of its known ability to biomineralize silica [37], other proteins and peptides have been found to be more effective in the biomineralization of TiO_2 under mild conditions. For example, a composite of bioengineered silicatein protein with silintaphin-1 as a scaffold protein was found to produce a mixture of the amorphous and anatase phase of TiO_2 at room temperature [83]. The protein silaffin and its analogues have been widely explored recently because of their ability to drive the formation of crystalline

TiO_2. In particular, the use of silaffin as a suitable protein additive was reported to produce the rutile phase at room temperature (Figure 4, left panel) [40]. However, the R5 peptide derived from silaffin produced mostly amorphous TiO_2 particles containing domains of the anatase and monoclinic phase at room temperature (Figure 4, right panel) [41,78,80], with annealing required to form anatase [78,79]. A composite of a Car9 silica-binding peptide fused with superfolder green fluorescent protein (sfGFP) was found to produce a mixture of amorphous and crystalline TiO_2 [81]. Interestingly, a similar composite of R5 fused with sfGFP in the same study was not effective at precipitating TiO_2 at room temperature, which led the authors to suggest that both the N- and C-termini of R5 must be free to induce TiO_2 mineralization [81], thus highlighting the key role of the chemical nature of the peptides and their interaction with Ti precursors.

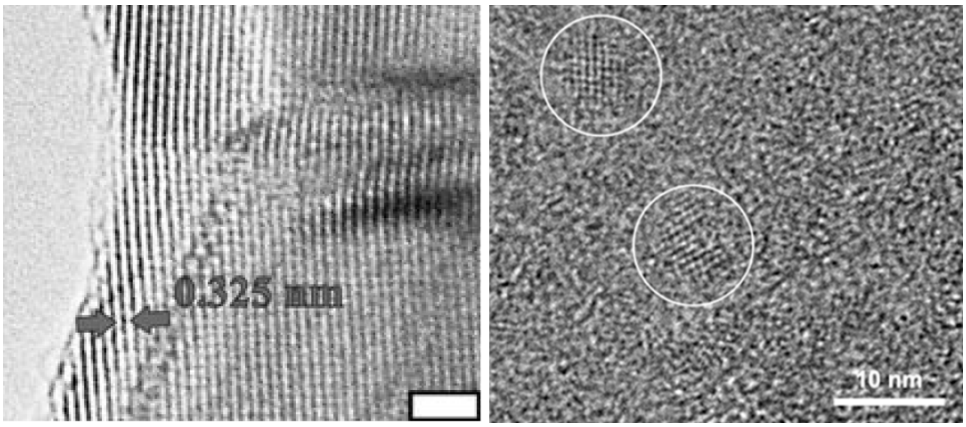

Figure 4. (**left**) High-resolution transmission electron microscope (HR-TEM) image of a fragment of a TiO_2 nanoparticle showing the (110) lattice fringes of rutile (the scale bar is 2 nm) (reproduced with permission from Ref. [40]); (**right**) HR-TEM image showing small crystalline domains (circled) with a size of a few nm^2 in the otherwise amorphous titania layer (reproduced with permission from Ref. [80]).

Similarly, several studies using small bio-additives, such as amino acid additives, have produced crystalline TiO_2 nanoparticles at room temperature [72,87]. For example, Yan et al. observed the conversion of amorphous titania to anatase after 30 days of aging at room temperature (without high-temperature annealing) and the appearance of rutile after 60 days of aging (Figure 5) [74]. Thus, while the goal of a fully controllable synthesis of crystalline TiO_2 phases at room temperature and within short timeframes has not yet been attained, the choice of the amino acid or protein additives offers a promising avenue to achieve this aim and is expected to be one of the key directions of future research.

Studies have also shown that the choice of amino acid additives can direct the formation of the crystalline phase of TiO_2. For example, a study by Shi et al. using TiBALDH as a precursor obtained the anatase phase at room temperature with arginine as an additive, but not with other amino acids such as serine, glycine, histidine or lysine [72].

Durupthy at al. found that the interactions of a $TiCl_4$ precursor with different amino acids resulted in different TiO_2 phases (Figure 6) [87]. In particular, the use of amino acids such as serine, glutamic acid or aspartic acid led to pure anatase phase formation. In contrast, histidine and proline additives produced mixtures of anatase with brookite, while glycine, lysine and arginine produced mixtures of anatase with rutile or with brookite, depending on the reaction pH. The initial formation of amorphous titania, prior to anatase formation, was attributed to preferential adsorption of the amino acids on the embryos of TiO_2, thus stabilising the amorphous particles and causing a delay in crystallisation. The formed amorphous titania then slowly converted to anatase after 1 week of aging [87]. The absence of the rutile phase in those cases was tentatively explained by the formation of [amino acid–Ti^{4+}] complexes which favoured anatase formation. The nucleation of anatase

in preference to rutile or brookite in reactions with aspartic acid, glutamic acid and serine was attributed to the specific attachment of these amino acids to the growing anatase facets, thus lowering the energies of these facets. The differences in adsorption of the amino acids on TiO_2 could be explained by the difference in the amino acids' pKa values [87]. This study opened the possibility of controlling the phase of crystalline TiO_2 particles through the choice of a suitable amino acid additive.

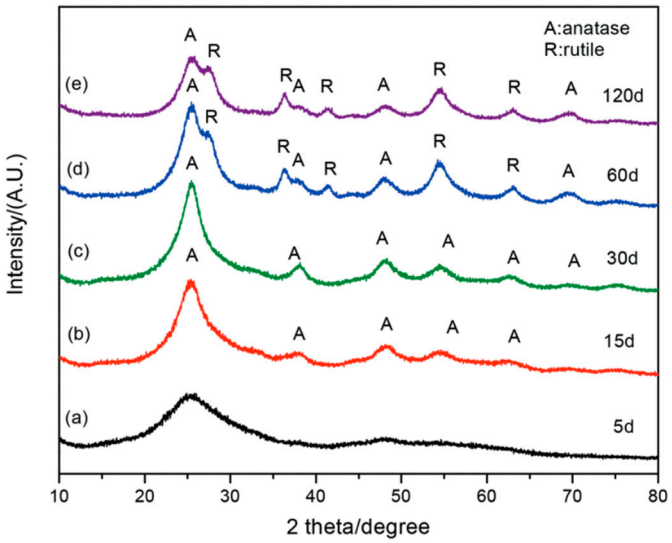

Figure 5. X-ray diffraction patterns of TiO_2 produced by polyamine-assisted synthesis after different reaction times: (**a**) 5 days, (**b**) 15 days, (**c**) 30 days, (**d**) 60 days and (**e**) 120 days (reproduced with permission from Ref. [74]).

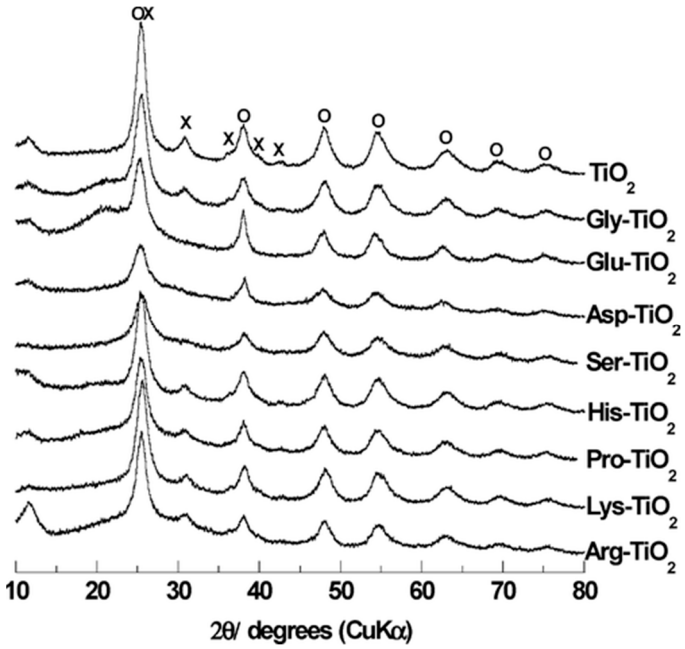

Figure 6. X-ray diffraction patterns of TiO_2 powders synthesised using different amino acid additives at pH of 4. Peaks marked with a circle correspond to anatase, while those marked with a cross correspond to brookite (reproduced with permission from Ref. [87]).

In another synthesis carried out under hydrothermal conditions, the amino acids aspartic acid and tyrosine yielded a pure anatase phase, whereas pure rutile was synthesised with alanine, glycine, proline, glutamic acid, serine, threonine, cystine and methionine.

However, lysine and arginine resulted in 70–80% of the brookite phase, while a higher concentration of lysine gave rise to pure brookite nanoparticles [68]. Thus, the choice of amino acid additives can direct TiO_2 synthesis towards desired phases, e.g., the anatase phase or the brookite phase, which are less stable but often display higher photocatalytic activity [18,19].

A protein-assisted TiO_2 synthesis study by Hellner et al. [81] similarly found that the nature and the ratio of the crystalline phases was dependent on the chemical nature of the peptide additives. This study considered several mutations to the Car9 peptide fused to the sfGFP protein. While the TiO_2 products were only partly crystalline, the amount of the crystalline phases increased when Car9 or its mutants were added to sfGFP; the mutations also tuned the ratio of the anatase and monoclinic bronze phase from 20%:80% to 65%:35% (Figure 7). The authors hypothesized that the catalytic action of the peptides was due to the peptides acting as ligands and displacing lactate ligands in the TiBALDH precursor, thus promoting polycondensation between adjacent Ti complexes. The tendency to form monoclinic crystals was attributed to favourable electrostatic interactions between positively charged side chains in peptides and negatively charged titania precursors, promoting the formation of compact monoclinic crystallites [81].

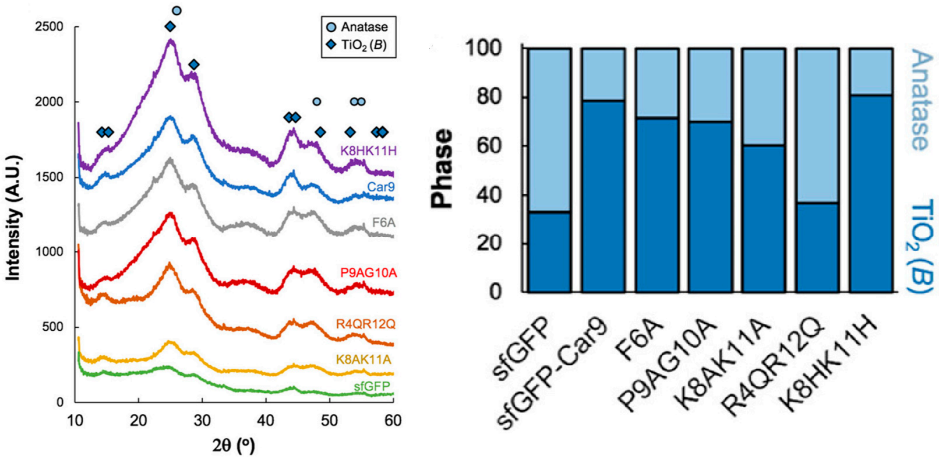

Figure 7. (**left**) X-ray diffraction patterns of TiO_2 powders precipitated using peptides fused to the sfGFP protein. Peaks corresponding to the anatase and monoclinic bronze TiO_2(B) phases are labelled with the circles and diamonds, respectively. (**right**) Fraction of anatase (light blue) to TiO_2(B) (dark blue) phase in nanocrystalline inclusions determined from XRD patterns (reproduced with permission from Ref. [81]).

The reasons for the preferential formation of particular TiO_2 phases were discussed in these studies using qualitative arguments. To gain a deeper understanding of how specific amino acids or amino acid sequences may drive the growth of different titania phases, future studies need to investigate the interactions between amino acids and growing TiO_2 particles; in particular, computational modelling studies are needed to obtain quantitative insights into the strength of amino acid–titania interactions.

3.2. Role of Bio-Inspired Additives as Templates and Capping Agents: Effect on Morphology

Amino acids, peptides and proteins can act as templates for oxide particle formation [101]. Beyond crystallinity and the crystal phase, properties such as the particle size, shape and surface area of synthesised TiO_2 can also be controlled by the selection of an appropriate additive. This is attributed to additives acting as capping agents, which form bonds to the growing crystal surfaces to control the growth in a particular direction of a crystal facet on the surface of a particle. This allows for the minimisation of interfacial tension and stabilisation of a particular facet [68,115].

For example, Kanie and Sugimoto first reported in 2004 that amino acids could be used as shape controllers in TiO_2 synthesis using $Ti(OH)_4$ gel at 140 °C (Figure 8) [115]. The shape

of the synthesised titanium dioxide particles relates to the abundance of particular crystal facets [22]. The dominance of a particular crystal facet in a synthesis was controlled by the concentration of the amino acids [115]. Moreover, the acidic or basic nature of the side groups of amino acids also affected the shape of the synthesised nanoparticles, as shown in Figure 8. For example, the basic amino acid lysine and neutral amino acids, such as glycine and serine, preferred to generate TiO_2 nanoparticles with rod-like shapes, whereas acidic amino acids such as aspartic or glutamic acid produced spindle-like nanostructures of TiO_2 [115].

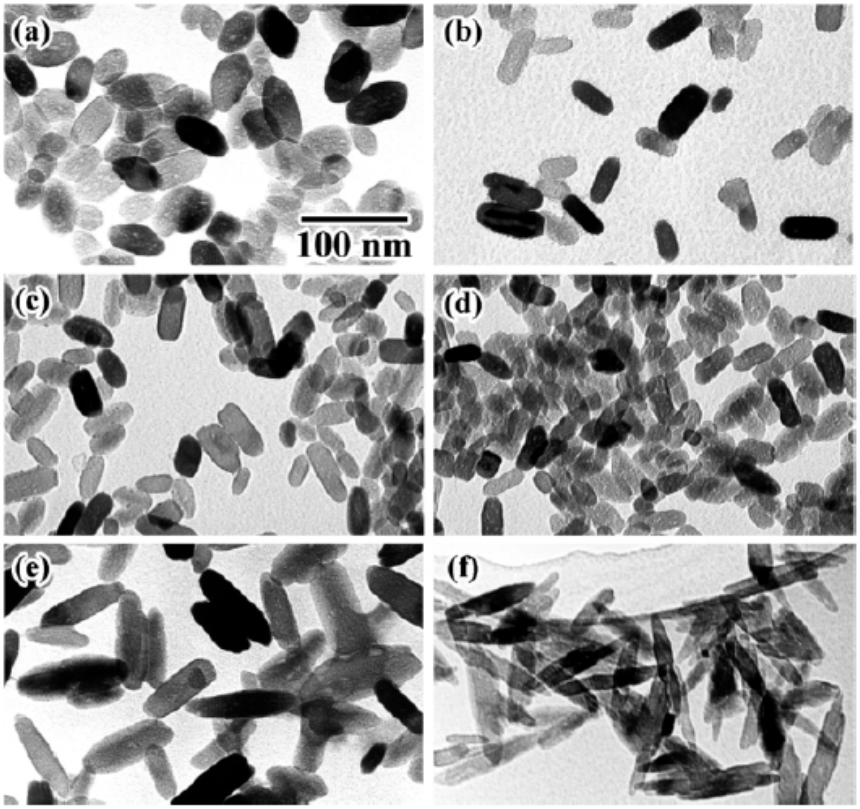

Figure 8. TEM images of TiO_2 synthesised (**a**) without amino acid additive; and with (**b**) glycine, (**c**) serine, (**d**) lysine, (**e**) aspartic acid and (**f**) glutamic acid (reproduced with permission from Ref. [115]).

Similarly, more complex bio-inspired additives involving peptides fused to the superfolder green fluorescent protein produced a variety of morphologies of TiO_2 nanoparticles, such as needles, threads, plates and peapods [96]. Furthermore, the morphology of TiO_2 products could be changed from large bulk-like monoliths to networks of small interconnected particles by controlling the diffusion in the reaction medium by increasing the amount of agarose hydrogel in the solution [96].

The templating effect of additives was also demonstrated in a study which used L-alanine and dodecylamine (DDA) additives with a titanium tetraisopropoxide precursor [112]. While the addition of alanine alone produced small (apx. 10 nm diameter) TiO_2 particles, the simultaneous addition of alanine and DDA resulted in particles with diameters between 300 and 700 nm. DDA was believed to act as a neutral surfactant controlling the size and shape of spherical TiO_2 particles (Figure 9), while alanine reacted with the Ti precursor and acted as a dopant to introduce nitrogen in the synthesized titania [112].

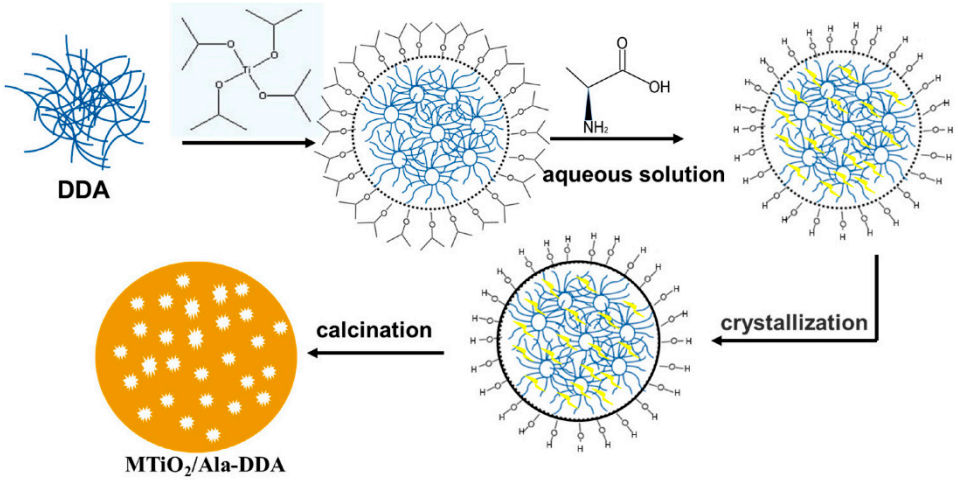

Figure 9. Schematic illustration of the mechanism of formation of mesoporous TiO_2 assisted by alanine (shown as yellow strands) and dodecylamine (DDA, shown as blue strands) additives (reproduced with permission from Ref. [112] licenced under CC BY 4.0).

The position of the amino group in the chain was also found to affect the particle size and photocatalytic performance of the synthesised nanoparticles; e.g., a comparison of α-alanine and β-alanine showed the formation of a dense forest of fine TiO_2 nanorods with α-alanine, whereas coarser nanorods with a lower density were observed with β-alanine [100]. Different amino acids were also reported to result in different mean particle sizes of as-synthesised TiO_2 between 2.5 and 8 nm, with the particle sizes dependent both on the nature of the amino acids and on the pH [87].

Moreover, a larger diameter of synthesised TiO_2 nanoparticles was obtained when using the glycylglycine peptide additive consisting of two glycine units compared to the glycine additive [100]. Furthermore, Bakre et al. reported that amino-acid-assisted synthesised TiO_2 anatase had a smaller particle size and crystallite size compared to commercial P25. Specifically, proline, valine and aspartic acid yielded smaller particle sizes of TiO_2 nanoparticles than other amino acids, such as glycine, alanine, glutamic acid and serine; these smaller particle sizes then resulted in an improved photocatalytic performance [101].

A pronounced effect on TiO_2 particle size was achieved using peptide additives that differed only in the ratio of serine (S) and lysine (K) residues [76]. The shorter KSSKK peptide precipitated spherical TiO_2–peptide composite particles with a mean diameter of 200 nm, while a longer peptide $SKSK_3SKS$ precipitated much larger spherical particles with a mean diameter of 510 nm (Figure 10). The precipitation kinetics also differed for the two peptide additives, saturating at very low peptide concentrations for the former peptide and occurring over a large range of concentrations for the latter. Complementary density functional theory calculations did not reveal strong differences in the binding of the S and K amino acid residues to TiO_2; therefore, the difference in precipitation was instead attributed to the different self-aggregation behaviours of the peptides themselves [76].

These studies demonstrate that the size and shape of TiO_2 particles can be controlled through the choice of amino acid or peptide additives. Different nanoparticle sizes are likely to be required for different applications: for example, small nanoparticle sizes of tens of nm are beneficial for photocatalysis [101], while applications as pigments require large sizes of about 250 nm [116]. In biomedical applications, small nanoparticle sizes are useful for drug delivery, as a small size facilitates cell membrane penetration; however, a larger nanoparticle size helps avoid cytotoxicity [117]. Therefore, developing targeted synthesis procedures that controllably produce nanoparticles of specific sizes is an important direction for technological applications of TiO_2.

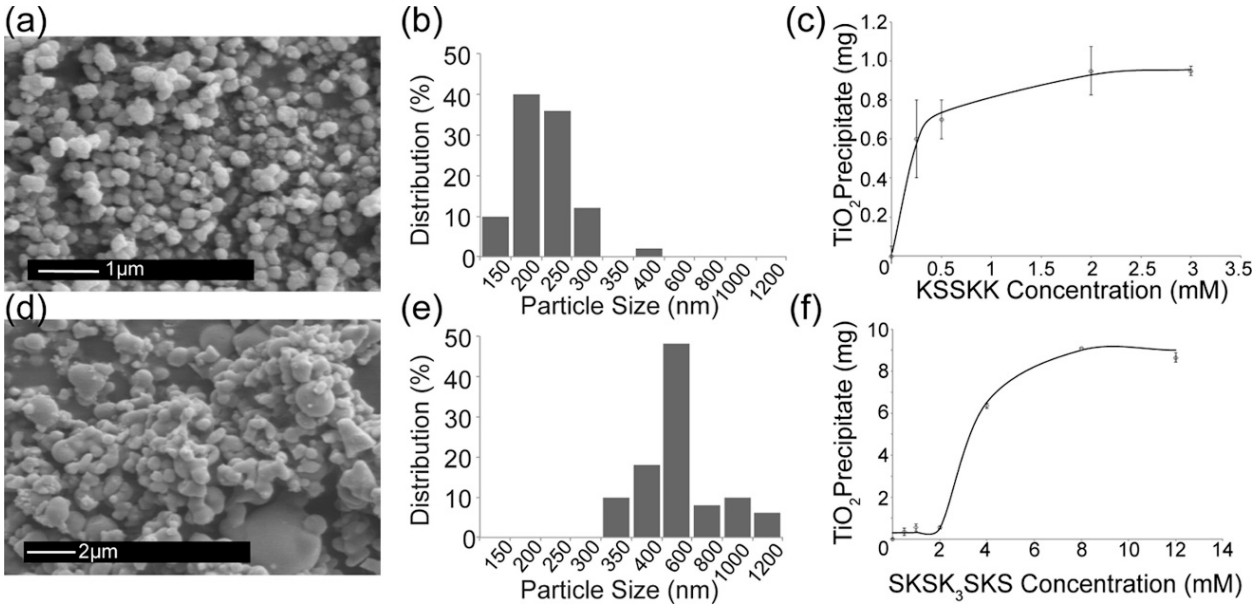

Figure 10. (**a**,**d**) Scanning electron microscope (SEM) images of TiO_2–peptide coprecipitate particles; (**b**,**e**) particle size distribution histograms; (**c**,**f**) TiO_2 precipitation as a function of peptide concentration. **Top** row: results for the KSKK peptide; **bottom** row: results for the $SKSK_3SKS$ peptide (reproduced with permission from Ref. [76]).

Finally, the removal of the template after the synthesis is a crucial step for obtaining pure TiO_2 products when conventional templates are used for the synthesis of hierarchical nanomaterials [34,118,119]. One of the benefits of calcination is that it helps to remove the organic templates. In case of bio-inspired additives, centrifuging and washing can be sufficient to remove the additives and can help avoid the calcination step [72].

3.3. Interactions of Bio-Additives with TiO_2

As summarised in Figure 1, bio-inspired additives, such as amino acids, play a multifunctional role: they initialise hydrolysis, and they can be used as catalysts, templates and capping agents in TiO_2 synthesis. They can influence the phase, shape, size and surface area of the synthesised TiO_2 nanoparticles. Going beyond the successful synthesis of TiO_2 with bio-inspired additives, a number of studies have investigated the nature of the interaction of amino acids with TiO_2 and their role in the mechanism of amino-acid-assisted TiO_2 synthesis [120–130]. Interactions of amino acids with Ti precursors and TiO_2 play a key role in understanding nanoparticle nucleation and growth mechanisms during amino-acid-assisted synthesis. These interactions are believed to be predominantly electrostatic [131], although other interactions, such as hydrogen bonds, can also be present [87]. The formation of hydrogen bonds between amine groups of amino acids and surface hydroxyl groups of the TiO_2 colloid was confirmed by infrared spectroscopy studies [101]. The adsorption of amino acids on TiO_2 crystal facets can affect the surface energy (interfacial tension) of these facets and stabilise particular crystal facets and/or particular polymorphs, such as anatase and brookite [87].

To understand the nature of interactions of amino acids with TiO_2, a number of experimental and theoretical studies on the adsorption of amino acids on TiO_2 have been carried out [120–130]. Since amino acids contain at least two functional groups (an amine group, a carboxylic group and a specific side group), their adsorption on TiO_2 is complex and depends on the nature of the amino acid, on the TiO_2 crystallographic surface and the extent of surface hydroxylation, and on the solution pH [120,122,123,126–130]. The studies showed that the binding of amino acids on dry (non-hydroxylated) TiO_2 surfaces occurs mainly via the carboxylic group binding to the surface Ti atoms [121,123,130], while amino acids in solution bind to the hydroxyl groups present on TiO_2 surfaces [120,128,129].

To gain a molecular-level understanding of the nature and strength of interactions of amino acids with TiO_2 surfaces, computational studies of amino acid adsorption were carried out using molecular dynamics [128,129] and density functional theory (DFT) [127,130] to compare the behaviour of basic and acidic amino acids (which are expected to be protonated or deprotonated, respectively, at a neutral pH). The adsorption of protonated amino acids, such as arginine and lysine, was found to be stronger as compared to that of deprotonated aspartic acid, both on the rutile (110) surface [128] and on the TiO_2 anatase (101) surface [127], both on the dry surfaces and in an aqueous environment [127]. A DFT study of multiple amino acids on dry rutile (110) and anatase (101) surfaces also found that polar amino acids were adsorbed more strongly than non-polar ones on both surfaces [130]. DFT calculations of amino acids on the anatase (101) surface (structures shown in Figure 11) found that the adsorption was 0.1–1.0 eV weaker on the hydrated surface compared to the dry surface; the reason for this large energy variation is that the calculated adsorption energies on the hydrated surface depended on the number of water molecules assigned to the amino acids' solvation shells [127]. Molecular dynamics calculations of free energies (incorporating both enthalpic and entropic effects) of arginine, lysine and aspartic acid on the dry and hydrated rutile (110) surfaces showed only slightly more favourable binding on the dry surfaces, showing that the effect of entropy must be taken into account when evaluating the strength of binding [128].

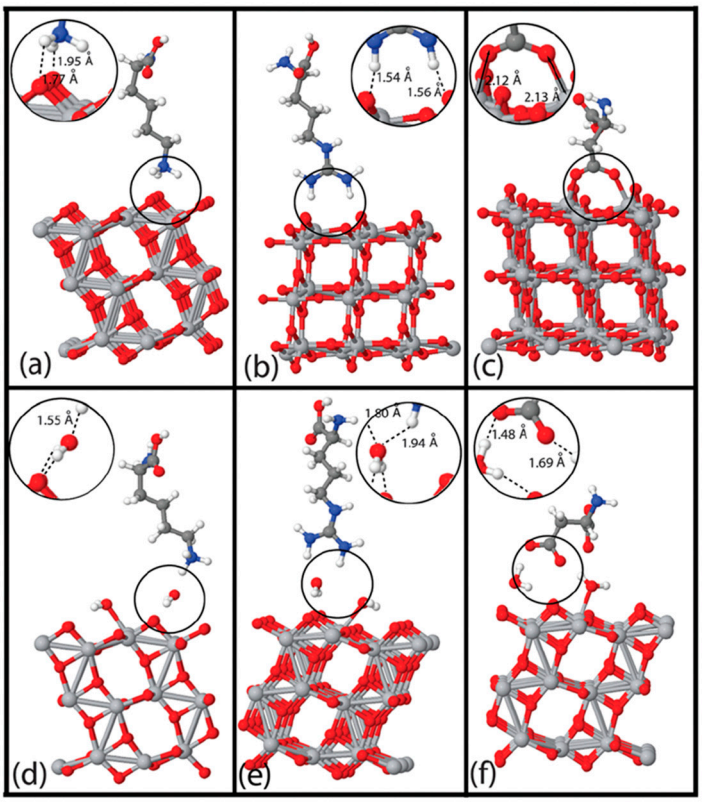

Figure 11. (**a**–**f**) Amino acid adsorption on the dry (**upper** panel) and hydrated (**lower** panel) TiO_2 anatase (101) surface: (**a**,**d**) arginine; (**b**,**e**) lysine; and (**c**,**f**) aspartic acid (reproduced with permission from Ref. [127]). Ti atoms are shown as light grey spheres, O atoms—red, C atoms—darker grey, N atoms—blue, H atoms—white spheres.

Understanding the interactions of amino acids with TiO_2 is insightful for determining the role of more complex bio-additives, such as peptides that comprise multiple amino acids. For example, Puddu et al. compared the performance of two different peptides, Ti-1 (QPYLFATDSLIK) and Ti-2 (GHTHYHAVRTQT), by analysing surface interactions of the constituent amino acids of the peptides with amphoteric surface groups on the titania

surface [41]. They found that the Ti-1 peptide provided faster kinetics in TiO_2 formation; this was explained by Ti-1 containing oppositely charged aspartic acid and lysine groups, which have a greater affinity towards the TiBALDH precursor than the Ti-2 peptide during the initial nucleation stage. However, Ti-2 was found to have a higher affinity towards the TiO_2 surface, because it contains several basic amino acids, which bind more strongly to the negatively charged TiO_2 surface groups at a neutral pH [41].

Thus, specific interactions between amino acids and TiO_2 govern the mechanisms, kinetics and thermodynamics of bio-inspired synthesis reactions. Furthermore, amino acid–TiO_2 interactions are relevant when amino acids are used as surface modifiers for TiO_2 functionalisation, e.g., to improve the photocatalytic activity of TiO_2 [132,133]. Moreover, bio-inspired additives, e.g., pre-polymerised dopamine, can also be used as growth inhibitors of TiO_2 nanoparticles, which enable size control as well as further functionalisation with more complex organic molecules [72].

The production of TiO_2 nanoparticles in a controllable manner rather than by trial and error requires a molecular-scale understanding of interactions at all stages of TiO_2 synthesis, from nucleation to growth and the termination of synthesis reactions. Theoretical modelling is indispensable to achieving this understanding. While calculations have already been used to investigate the strength of the binding of amino acids and peptides to TiO_2 [127–130], further insights from modelling are needed: for example, exploring the interactions of Ti precursors and growing nuclei with molecular additives will help us understand the key structural factors responsible for TiO_2 phases, shapes and reaction kinetics.

4. Photocatalytic Performance of TiO_2 Synthesised via Bio-Inspired Route

Photocatalysis is one of the key applications for titanium dioxide. By considering the relationship between material, process, property and performance (MP^3), synthesis process parameters have a direct influence on the photocatalytic performance of synthesised TiO_2. For example, the selection of a suitable precursor material can improve the photocatalyst's performance: e.g., TiO_2 made from the TiBALDH precursor showed better levels of stability and photocatalytic performance compared to TiO_2 made from Ti isopropoxide [64,134].

Table 3 provides examples of TiO_2 photocatalysts synthesised by bio-inspired routes and their photocatalytic performance. Industrial pollutants, including textile dyes such as rhodamine B, methyl orange, methylene blue, alizarin red, malachite green and crystal violet, have been degraded using bio-inspired synthesised TiO_2 on the laboratory scale [71,83,88,93,101,102]. Although bio-inspired additives do not directly participate in the photocatalytic degradation process, bio-inspired synthesis processes enable the control of the phase, morphology and size of as-synthesised TiO_2 particles and therefore can indirectly influence the photocatalytic performance. For example, the photocatalytic activity of TiO_2 produced by bio-inspired synthesis was found to be superior compared to a commercial P25 TiO_2 photocatalyst and TiO_2 synthesized without bio-additives [88,101,135,136].

Table 3. Photocatalytic performance of bio-inspired synthesised TiO_2.

Material	Precursor	Additive	Photocatalytic Process	Photocatalytic Performance	Ref.
TiO_2 nanofibers	$TiCl_4$	Pomelo peel	Degradation of methyl orange (MO), rhodamine B, reactive brilliant blue, malachite green	Better photocatalytic activity than commercial P25 TiO_2. Up to 99% degradation of MO in 30 min	[88]
TiO_2 nanoparticles	$TiCl_4$	Jatropha leaf extract	Degradation of tannery wastewater	82% removal of chemical oxygen demand COD; 76% removal of Cr^{+6}	[137]
Mesoporous TiO_2 photocatalysts	Tetra butyl titanate ($Ti(OBu)_4$)	Pollen grains	Degradation of rhodamine B	95% degradation after 120 min	[90]
TiO_2 nanoparticles	Ti isopropoxide ($Ti(Oi\text{-}Pr)_4$)	Aloe vera gel	Degradation of picric acid	Complete degradation in 120 min	[91]

Table 3. *Cont.*

Material	Precursor	Additive	Photocatalytic Process	Photocatalytic Performance	Ref.
TiO_2 nanohybrids	TiO_4	Parthenium hysterophorus	Degradation of methylene blue (MB), crystal violet (CV), methyl orange (MO), alizarin red (AR)	In 6 h: degradation in (%) 92.5 MB, 81.5 MO, 79.7 CV, 77.3 AR	[93]
Indium-modified TiO_2 composite with tobacco stem silk	Tetra butyl titanate	Tobacco stem silk	Degradation of tetracycline hydrochloride (TCH)	92.9% removal efficiency in 90 min under visible light	[138]
Graphene-supported g-C_3N_4/TiO_4 hetero-aerogels	Ti-BALDH	KIIIIKYWYAF peptide	Degradation of methylene blue, rhodamine B (RhB)	MB: 97% in 120 min; RhB: 60% in 120 min	[77]
g-C_3N_4/TiO_2	Ti-BALDH	Arginine	Degradation of rhodamine B, phenol	Rhodamine B 84% degraded in 5 h; Phenol 76% degradation in 120 min	[71]
Mesoporous nano TiO_2	Ti isopropoxide	Various amino acids	Degradation of methylene blue, calmagite	Almost complete degradation. Samples prepared with proline, valine and aspartic acid resulted in better degradation activity than P25 TiO_2.	[101]
TiO_2 hierarchical spheres	Tetra butyl titanate	Glycine	Degradation of methyl orange (MO)	98% degradation of MO in 30 min	[102]
L-hydroproline modified TiO_2	$TiCl_4$	L-hydroproline	Degradation of rhodamine B	97% degradation in 4 h, better performance than pure TiO_2, visible light activity	[135]
Amino-acid-modified TiO_2	Tetra butyl titanate	L-proline, L-arginine, L-methionine	Degradation of methyl orange (MO), direct red 16 DR16	MO removal: 95% DR16 removal: 97% in 60 min	[139]
Amino-acid-modified TiO_2	Tetra butyl titanate	L-proline, L-arginine, L-methionine	Degradation of metronidazole, cephalexin	Metronidazole removal: 99.9% (TOC removal: 81%) Cephalexin removal: 97.2% (TOC removal: 75%)	[140]
CdS/Au/N-doped TiO_2 heterostructure	$TiCl_3$	Cherry blossom leaves	Hydrogen production	H_2 evolution activity higher than P25 or TiO_2 synthesized without template	[141]
Templated TiO_2	$TiCl_3$	Olive leaves	Hydrogen production	H_2 evolution activity 64% higher than P25 under solar light and 144% higher under UV light	[65]
Templated mesoporous TiO_2	$TiCl_3$	Camellia tree leaves	CO_2 reduction	Higher yield of CO + CH_4, higher selectivity towards CH_4 than towards P25	[66]
TiO_2 rutile and brookite nanoparticles	Peroxo-titanic acid	Various amino acids	CO_2 reduction	Brookite synthesised in the presence of Lys showed the highest photocatalytic activity	[68]

One of the limitations of the pure TiO_2 photocatalyst is that it can only function under UV light irradiation. However, with the bio-inspired route, further enhancements in its photocatalytic activity and biocompatibility can be achieved by modifying the surface of TiO_2 with bio-inspired additives, such as the amino acids glycine, hydroxyproline or tyrosine [133,135,136], which can reduce the bandgap of the TiO_2–amino acid composite, as shown in Figure 12 for a TiO_2–tyrosine composite [136].

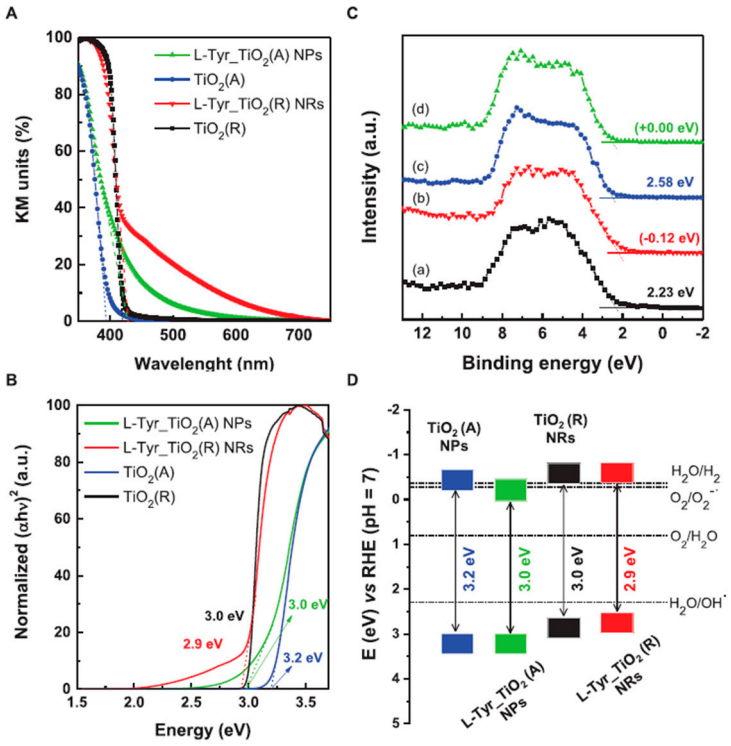

Figure 12. (**A**) Diffuse reflectance UV spectra or TiO_2 rutile nanorods (NRs) and anatase nanoparticles (NPs) with and without L-tyrosine, (**B**) estimation of the optical gap of these materials from Tauc plots, (**C**) X-ray photoemission spectra in the valence band region, (**D**) schematic of band positions of pyre- and tyrosine-modified TiO_2 nanomaterials (reproduced with permission from Ref. [136]).

Surface coating with bio-inspired materials hinders the agglomeration of TiO_2 nanoparticles. Thus, TiO_2 nanoparticles coated with L-valine, L-leucine, L-isoleucine and L-methionine displayed reduced agglomeration [142]. This provides a greater surface area for interactions with pollutants and light absorption.

In summary, there are several ways in which bio-inspired additives can contribute to the photocatalytic activity of TiO_2 nanomaterials: (1) their use as an additive in the nano-TiO_2 synthesis reaction; and (2) their use for the surface functionalisation of TiO_2.

In the first aspect, when the bio-inspired additives are added to the synthesis reaction, they provide process benefits, such as carrying out the synthesis reaction at mild conditions and controlling TiO_2 particles' phase, size and shape. TiO_2 synthesised with bio-inspired additives can form nanoparticles with a higher surface area to volume ratio, which are suitable for photocatalytic applications. In the second aspect, when the bio-additives are used as surface modifiers for TiO_2 nanoparticles, they can increase light absorption and improve the photocatalytic activity by enabling light harvesting in the visible region, thus improving the pollutant degradation performance of the TiO_2 photocatalyst.

In both of these aspects, the interactions of bio-additives, such as amino acids and proteins, with the surface of TiO_2 particles are important. In bio-inspired synthesis, the influence of these interactions on the properties is indirect, as bio-additives help control the growth of the synthesised nucleus of TiO_2 by acting as surfactants, templates and capping agents and, ultimately, as size and shape controllers. Thus, they determine the surface-area-to-volume ratio and can lead to a larger surface area for better light absorption and pollutant adsorption. In comparison, in surface functionalisation, the interactions are directly influencing the properties of the produced composite material by creating additional energy levels to enable the absorption of light in a broader spectral range and thus to facilitate photocatalysis activated by visible light.

5. Conclusions

This review highlights the role of bio-inspired additives as crucial ingredients in the synthesis of titanium dioxide, which have great potential for controlling the phase, shape and size of TiO_2 nanoparticles for specific applications, in particular for the photocatalytic degradation of pollutants. Various biomolecules, such as proteins, peptides and amino acids, have been used with different Ti precursors to successfully synthesise crystalline or amorphous TiO_2. Amino acids, as relatively simple bio-inspired additives, have also been the subject of mechanistic studies to elucidate their role in the synthesis of TiO_2. However, the key process challenges to design a green synthesis method still remain unresolved.

The key challenges and hence potential opportunities for future research in the green synthesis of TiO_2 can be summarised as follows, which are broadly based on a recently developed multi-criteria discovery, design and manufacturing framework [45]:

1. Obtaining desired critical quality attributes (CQAs) such as the crystallinity and morphology of titanium dioxide suitable for desired applications, such as photocatalysis;
2. Carrying out synthesis under mild conditions, ideally at room temperature;
3. Assessing the economics and sustainability of bio-inspired synthesis methods;
4. Up-scaling the methods of the green synthesis of TiO_2 for industrial production.

We conclude the review by discussing potential solutions to these challenges.

(1) As seen from the examples discussed in this review, progress has already been made in addressing the first of these challenges: bio-inspired additives have enabled the synthesis of specific phases and morphologies of titania nanoparticles. However, the investigations so far have used the trial-and-error approach rather than systematic explorations informed by an understanding of titania–biomolecule interactions. Further, these studies have not focussed on the CQAs needed for desired applications. To identify molecular additives that controllably produce the desired CQAs, such as TiO_2 phase and morphology, several complementary approaches should be undertaken.

First, computational investigations of amino-acid-assisted synthesis reactions are needed in order to understand the mechanisms of bio–inorganic interactions and design new efficient bio-inspired additives. The computational studies so far have investigated the binding of amino acids on TiO_2 surfaces [127–130]. Future directions should go beyond simple binding to explore reaction processes, similar to the multiscale modelling studies of the bio-inspired synthesis of silica [143].

Second, the design of experiments approach should be utilised, which seeks relationships between process variables (e.g., concentrations of reactants) and response variables (e.g., product yield) as well as performance-oriented CQAs [144–146].

Third, machine learning, which has emerged as a powerful technique for identifying trends in data and developing predictive models for synthesis planning [147,148], should be applied to TiO_2 synthesis. For example, design of experiments has been applied to the sol-gel synthesis of TiO_2 [149,150], while machine learning has been used to optimize the synthesis of doped TiO_2 for photocatalytic applications [151] and to investigate the effect of synthesis parameters on the size and shape of TiO_2 obtained by hydrothermal synthesis [152]. This multi-pronged approach would help reach the final goal of developing standardised synthesis protocols (Ti precursor, molecular additives, solvent, pH and temperature) for producing TiO_2 nanoparticles with well-defined sizes and phase compositions.

(2) The key challenge in the state-of-the-art solution synthesis of titanium dioxide is obtaining the desired crystallinity and morphology of the titanium dioxide at room temperature. Studies that report the synthesis of titanium dioxide at room temperature require a long time (up to several days [74,87]). Thus, reducing the reaction time while keeping the reactions at mild conditions remains an important goal. Titanium dioxide synthesised and obtained at room temperature still does not necessarily have the required crystallinity, and post-synthesis heat treatment is required in most cases to achieve crystalline TiO_2. These post-synthesis heat treatments are carried out at high temperatures, typically above 450 °C.

The aim for the sustainable synthesis of TiO_2 remains to precipitate crystalline titanium dioxide at low temperatures and mild conditions.

The same three strands of exploration—computational modelling of TiO_2–biomolecule interactions to guide the choice of additives, the use of the design of experiments approach and machine learning analyses—should be applied in the search for additives that enable the low-temperature synthesis of crystalline TiO_2. At present, this area is underdeveloped, with very few examples of crystalline TiO_2 obtained at room temperature [40,72,74,87] and few examples of mixtures of amorphous and crystalline TiO_2 [41,75,76,81,83]. Based on the current knowledge, it is impossible to say conclusively whether small-molecule additives, such as amino acids, or larger additives, such as peptides, are more effective for the low-temperature synthesis of TiO_2. Finding an answer to this question requires a combination of "bottom-up" studies involving large-scale screening of multiple amino acids, and short peptide additives and "top-down" studies starting with protein additives, such as silaffin (the most successful additive for the room-temperature synthesis of TiO_2 [40]), and systematically exploring smaller fragments of these proteins. Such systematic studies can then be combined with machine learning analyses to identify peptide sequences that are effective at driving TiO_2 synthesis at low temperatures.

(3) An important point to consider is how economical, sustainable or green the bio-inspired synthesis methods are [77]. Compared to the conventional surfactants and capping agents used in the synthesis of nanomaterials, bio-inspired additives promise environmentally benign alternatives [39]. To assess this, it will be necessary to perform quantitative assessments of the bio-inspired additives and bio-assisted synthesis approaches. While a full life-cycle analysis is ideal, it can present significant practical barriers due to the lack of desired data on yields, conversions, reaction rates, etc. Simpler alternatives are being developed, such as the quantification based on the 12 principles of green chemistry. For example, a tool called DOZN^{TM} has been recently developed [153] and applied to nanomaterial synthesis [154]—such tools can rapidly provide an early-stage evaluation of "greenness", which can direct the researchers in selecting and identifying greener routes to titania synthesis.

(4) Finally, the challenge for the industrial production of TiO_2 is to scale-up the methods of green synthesis. During the synthesis stage, it is often believed that scale-up challenges are either separate to the discovery stage or trivial to solve, or both. Actually, it is neither of these, because decisions made at the discovery stage, e.g., the choice of solvents and conditions, can have profound effects on scalability and can even render some syntheses inherently non-scalable. Further, while reaction rates/chemical kinetics do not change with up-scaling, transport properties (mixing, heat and mass transfer) change with scale and in a non-linear fashion [155]. Here, lessons learned from the large-scale synthesis of other relevant materials can be used, considering factors such as reactor design, reagent mixing and product separation [156–158], as well as evaluating the technoeconomics, availability and toxicity of reagents [158–161].

In conclusion, resolving these challenges offers the tantalising prospect of the low-cost, large-scale bio-inspired synthesis of high-value TiO_2 with desired structures and properties that are suitable for diverse applications. As described above, future research should take a holistic approach and embrace multidisciplinary collaborations spanning experiments, modelling and novel mathematical and statistical tools.

Supplementary Materials: The following supporting information can be downloaded at: https://www.mdpi.com/article/10.3390/catal14110742/s1, Table S1: TiO_2 synthesis from $TiCl_4$ precursor; Table S2: TiO_2 synthesis from Ti alkoxide precursors. Refs. [162–175] are cited in the Supplementary Materials.

Author Contributions: Conceptualization, M.R.M., S.V.P. and N.M.; investigation, M.R.M.; data curation, M.R.M.; writing—original draft preparation, M.R.M.; writing—review and editing, N.M. and S.V.P.; supervision, N.M. and S.V.P.; project administration, N.M.; funding acquisition, N.M. and S.V.P. All authors have read and agreed to the published version of the manuscript.

Funding: This research was funded by the Grantham Centre for Sustainable Futures (Ph.D. studentship and training for M.R.M.). S.V.P. thanks for funding from EPSRC Fellowship (EP/R025983/1) for this work.

Data Availability Statement: No new data were created in this study.

Acknowledgments: M.R.M. would like to thank the Green Nanomaterials Group at the Department of Chemical and Biological Engineering and the Theory Group at the Department of Chemistry at the University of Sheffield for their useful discussions throughout the course of M.R.M.'s Ph.D, and to acknowledge brainstorming sessions at the SynBIM symposium (University of Manchester, 2020).

Conflicts of Interest: The authors declare no conflicts of interest. The funders had no role in the design of the study; in the collection, analyses, or interpretation of data; in the writing of the manuscript; or in the decision to publish the results.

References

1. Kudo, A.; Miseki, Y. Heterogeneous photocatalyst materials for water splitting. *Chem. Soc. Rev.* **2009**, *38*, 253–278. [CrossRef] [PubMed]
2. Friedmann, D.; Hakki, A.; Kim, H.; Choi, W.; Bahnemann, D. Heterogeneous photocatalytic organic synthesis: State-of-the-art and future perspectives. *Green Chem.* **2016**, *18*, 5391–5411. [CrossRef]
3. Fang, S.; Rahaman, M.; Bharti, J.; Reisner, E.; Robert, M.; Ozin, G.A.; Hu, Y.H. Photocatalytic CO_2 reduction. *Nat. Rev. Methods Primers* **2023**, *3*, 61. [CrossRef]
4. Melchionna, M.; Fornasiero, P. Updates on the Roadmap for Photocatalysis. *ACS Catal.* **2020**, *10*, 5493–5501. [CrossRef]
5. Chong, M.N.; Jin, B.; Chow, C.W.K.; Saint, C. Recent developments in photocatalytic water treatment technology: A review. *Water Res.* **2010**, *44*, 2997–3027. [CrossRef] [PubMed]
6. Mulay, M.R.; Martsinovich, N. TiO_2 Photocatalysts for Degradation of Micropollutants in Water. In *Clean Water and Sanitation*; Leal Filho, W., Azul, A.M., Brandli, L., Lange Salvia, A., Wall, T., Eds.; Springer International Publishing: Cham, Switzerland, 2021; pp. 1–19. [CrossRef]
7. Gupta, V.K.; Ali, I.; Saleh, T.A.; Nayak, A.; Agarwal, S. Chemical treatment technologies for waste-water recycling—An overview. *Rsc Adv.* **2012**, *2*, 6380–6388. [CrossRef]
8. Muñoz, I.; Peral, J.; Ayllón, J.A.; Malato, S.; Passarinho, P.; Domènech, X. Life cycle assessment of a coupled solar photocatalytic–biological process for wastewater treatment. *Water Res.* **2006**, *40*, 3533–3540. [CrossRef]
9. Pesqueira, J.F.; Pereira, M.F.R.; Silva, A.M. A life cycle assessment of solar-based treatments (H_2O_2, TiO_2 photocatalysis, circumneutral photo-Fenton) for the removal of organic micropollutants. *Sci. Total Environ.* **2021**, *761*, 143258. [CrossRef]
10. Magdy, M.; Alalm, M.G.; El-Etriby, H.K. Comparative life cycle assessment of five chemical methods for removal of phenol and its transformation products. *J. Clean. Prod.* **2021**, *291*, 125923. [CrossRef]
11. Caramazana-Gonzalez, P.; Dunne, P.W.; Gimeno-Fabra, M.; Zilka, M.; Ticha, M.; Stieberova, B.; Freiberg, F.; McKechnie, J.; Lester, E. Assessing the life cycle environmental impacts of titania nanoparticle production by continuous flow solvo/hydrothermal syntheses. *Green Chem.* **2017**, *19*, 1536–1547. [CrossRef]
12. Wu, F.; Zhou, Z.; Hicks, A.L. Life cycle impact of titanium dioxide nanoparticle synthesis through physical, chemical, and biological routes. *Environ. Sci. Technol.* **2019**, *53*, 4078–4087. [CrossRef] [PubMed]
13. Nakata, K.; Fujishima, A. TiO_2 photocatalysis: Design and applications. *J. Photochem. Photobiol. C Photochem. Rev.* **2012**, *13*, 169–189.
14. Armaković, S.J.; Savanović, M.M.; Armaković, S. Titanium Dioxide as the Most Used Photocatalyst for Water Purification: An Overview. *Catalysts* **2023**, *13*, 26.
15. Fujishima, A.; Honda, K. Electrochemical photolysis of water at a semiconductor electrode. *Nature* **1972**, *238*, 37. [CrossRef]
16. Schneider, J.; Matsuoka, M.; Takeuchi, M.; Zhang, J.; Horiuchi, Y.; Anpo, M.; Bahnemann, D.W. Understanding TiO_2 Photocatalysis: Mechanisms and Materials. *Chem. Rev.* **2014**, *114*, 9919–9986. [CrossRef] [PubMed]
17. Hernández-Alonso, M.D.; Fresno, F.; Suárez, S.; Coronado, J.M. Development of alternative photocatalysts to TiO_2: Challenges and opportunities. *Energy Environ. Sci.* **2009**, *2*, 1231–1257.
18. Kandiel, T.A.; Robben, L.; Alkaima, A.; Bahnemann, D. Brookite versus anatase TiO_2 photocatalysts: Phase transformations and photocatalytic activities. *Photochem. Photobiol. Sci.* **2013**, *12*, 602–609. [CrossRef]
19. Zhang, J.; Zhou, P.; Liu, J.; Yu, J. New understanding of the difference of photocatalytic activity among anatase, rutile and brookite TiO_2. *Phys. Chem. Chem. Phys.* **2014**, *16*, 20382–20386. [CrossRef]
20. Luttrell, T.; Halpegamage, S.; Tao, J.; Kramer, A.; Sutter, E.; Batzill, M. Why is anatase a better photocatalyst than rutile?—Model studies on epitaxial TiO_2 films. *Sci. Rep.* **2014**, *4*, 4043. [CrossRef]
21. Rej, S.; Hejazi, S.H.; Badura, Z.k.; Zoppellaro, G.; Kalytchuk, S.; Kment, S.; Fornasiero, P.; Naldoni, A. Light-induced defect formation and Pt single atoms synergistically boost photocatalytic H2 production in 2D TiO_2-bronze nanosheets. *ACS Sustain. Chem. Eng.* **2022**, *10*, 17286–17296. [CrossRef]

22. Katal, R.; Masudy-Panah, S.; Tanhaei, M.; Farahani, M.H.D.A.; Jiangyong, H. A review on the synthesis of the various types of anatase TiO_2 facets and their applications for photocatalysis. *Chem. Eng. J.* **2020**, *384*, 123384. [CrossRef]
23. Dong, H.; Zeng, G.; Tang, L.; Fan, C.; Zhang, C.; He, X.; He, Y. An overview on limitations of TiO_2-based particles for photocatalytic degradation of organic pollutants and the corresponding countermeasures. *Water Res.* **2015**, *79*, 128–146. [CrossRef] [PubMed]
24. Gupta, S.M.; Tripathi, M. A review on the synthesis of TiO_2 nanoparticles by solution route. *Cent. Eur. J. Chem.* **2012**, *10*, 279–294. [CrossRef]
25. Han, X.-H.; Li, C.-Q.; Tang, P.; Feng, C.-X.; Yue, X.-Z.; Zhang, W.-L. Solid-Phase Synthesis of Titanium Dioxide Micro-Nanostructures. *ACS Omega* **2022**, *7*, 35538–35544. [CrossRef]
26. Khan, S.; Katsumata, K.-i.; Rodríguez-González, V.; Terashima, C.; Fujishima, A. Gas-Phase Synthesis for Mass Production of TiO2 Nanoparticles for Environmental Applications. In *Handbook of Nanomaterials and Nanocomposites for Energy and Environmental Applications*; Kharissova, O.V., Torres-Martínez, L.M., Kharisov, B.I., Eds.; Springer International Publishing: Cham, Switzerland, 2021; pp. 953–973. [CrossRef]
27. Wu, J.-M.; Shih, H.C.; Wu, W.-T.; Tseng, Y.-K.; Chen, I.C. Thermal evaporation growth and the luminescence property of TiO_2 nanowires. *J. Cryst. Growth* **2005**, *281*, 384–390. [CrossRef]
28. Samal, S. Synthesis of TiO_2 Nanoparticles from Ilmenite Through the Mechanism of Vapor-Phase Reaction Process by Thermal Plasma Technology. *J. Mater. Eng. Perform.* **2018**, *27*, 2622–2628. [CrossRef]
29. Heo, C.H.; Lee, S.-B.; Boo, J.-H. Deposition of TiO_2 thin films using RF magnetron sputtering method and study of their surface characteristics. *Thin Solid Film.* **2005**, *475*, 183–188. [CrossRef]
30. Saraf, L.V.; Patil, S.I.; Ogale, S.B.; Sainkar, S.R.; Kshirsager, S.T. Synthesis of nanophase TiO2 by ion beam sputtering and cold condensation technique. *Int. J. Mod. Phys. B* **1998**, *12*, 2635–2647. [CrossRef]
31. Lee, H.; Song, M.Y.; Jurng, J.; Park, Y.-K. The synthesis and coating process of TiO_2 nanoparticles using CVD process. *Powder Technol.* **2011**, *214*, 64–68. [CrossRef]
32. Bessergenev, V.G.; Khmelinskii, I.V.; Pereira, R.J.F.; Krisuk, V.V.; Turgambaeva, A.E.; Igumenov, I.K. Preparation of TiO_2 films by CVD method and its electrical, structural and optical properties. *Vacuum* **2002**, *64*, 275–279. [CrossRef]
33. Goossens, A.; Maloney, E.L.; Schoonman, J. Gas-phase synthesis of nanostructured anatase TiO_2. *Chem. Vap. Depos.* **1998**, *4*, 109–114. [CrossRef]
34. Cargnello, M.; Gordon, T.R.; Murray, C.B. Solution-phase synthesis of titanium dioxide nanoparticles and nanocrystals. *Chem. Rev.* **2014**, *114*, 9319–9345. [CrossRef] [PubMed]
35. Ragadhita, R.; Nandiyanto, A.B.D.; Maulana, A.C.; Oktiani, R.; Sukmafitri, A.; Machmud, A.; Surachman, E. Techno-economic analysis for the production of titanium dioxide nanoparticle produced by liquid-phase synthesis method. *J. Eng. Sci. Technol.* **2019**, *14*, 1639–1652.
36. Anastas, P.T.; Warner, J.C. Principles of green chemistry. In *Green Chemistry: Theory and Practice*; Oxford University Press: New York, NY, USA, 1998; pp. 29–56.
37. Sumerel, J.L.; Yang, W.; Kisailus, D.; Weaver, J.C.; Choi, J.H.; Morse, D.E. Biocatalytically templated synthesis of titanium dioxide. *Chem. Mater.* **2003**, *15*, 4804–4809. [CrossRef]
38. Mann, S. *Biomineralization: Principles and Concepts in Bioinorganic Materials Chemistry*; Oxford University Press: Oxford, UK, 2001.
39. Patwardhan, S.V.; Manning, J.R.; Chiacchia, M. Bioinspired synthesis as a potential green method for the preparation of nanomaterials: Opportunities and challenges. *Curr. Opin. Green Sustain. Chem.* **2018**, *12*, 110–116. [CrossRef]
40. Kröger, N.; Dickerson, M.B.; Ahmad, G.; Cai, Y.; Haluska, M.S.; Sandhage, K.H.; Poulsen, N.; Sheppard, V.C. Bioenabled synthesis of rutile (TiO_2) at ambient temperature and neutral pH. *Angew. Chem. Int. Ed.* **2006**, *45*, 7239–7243. [CrossRef]
41. Puddu, V.; Slocik, J.M.; Naik, R.R.; Perry, C.C. Titania binding peptides as templates in the biomimetic synthesis of stable titania nanosols: Insight into the role of buffers in peptide-mediated mineralization. *Langmuir* **2013**, *29*, 9464–9472. [CrossRef]
42. Banerjee, I.A.; Yu, L.; Matsui, H. Cu nanocrystal growth on peptide nanotubes by biomineralization: Size control of Cu nanocrystals by tuning peptide conformation. *Proc. Natl. Acad. Sci. USA* **2003**, *100*, 14678–14682. [CrossRef]
43. Sano, K.-I.; Sasaki, H.; Shiba, K. Specificity and biomineralization activities of Ti-binding peptide-1 (TBP-1). *Langmuir* **2005**, *21*, 3090–3095. [CrossRef]
44. Patwardhan, S.V.; Staniland, S.S. *Green Nanomaterials*; IOP Publishing: Bristol, UK, 2019.
45. Pilling, R.; Coles, S.R.; Knecht, M.R.; Patwardhan, S.V. Multi-criteria discovery, design and manufacturing to realise nanomaterial potential. *Commun. Eng.* **2023**, *2*, 78. [CrossRef]
46. Langa, C.; Hintsho-Mbita, N.C. Plant and bacteria mediated synthesis of TiO_2 NPs for dye degradation in water. A review. *Chem. Phys. Impact* **2023**, *7*, 100293. [CrossRef]
47. Rajaram, P.; Jeice, A.R.; Jayakumar, K. Review of green synthesized TiO_2 nanoparticles for diverse applications. *Surf. Interfaces* **2023**, *39*, 102912. [CrossRef]
48. Sagadevan, S.; Imteyaz, S.; Murugan, B.; Lett, J.A.; Sridewi, N.; Weldegebrieal, G.K.; Fatimah, I.; Oh, W.-C. A comprehensive review on green synthesis of titanium dioxide nanoparticles and their diverse biomedical applications. *Green Process. Synth.* **2022**, *11*, 44–63. [CrossRef]
49. Verma, V.; Al-Dossari, M.; Singh, J.; Rawat, M.; Kordy, M.G.; Shaban, M. A review on green synthesis of TiO2 NPs: Photocatalysis and antimicrobial applications. *Polymers* **2022**, *14*, 1444. [CrossRef] [PubMed]

50. Wang, W.; Gu, B.; Liang, L.; Hamilton, W.A.; Wesolowski, D.J. Synthesis of rutile (α-TiO_2) nanocrystals with controlled size and shape by low-temperature hydrolysis: Effects of solvent composition. *J. Phys. Chem. B* **2004**, *108*, 14789–14792. [CrossRef]
51. Collins, A. *Nanotechnology Cookbook: Practical, Reliable and Jargon-Free Experimental Procedures*; Elsevier: Amsterdam, The Netherlands, 2012.
52. Gordon, T.R.; Cargnello, M.; Paik, T.; Mangolini, F.; Weber, R.T.; Fornasiero, P.; Murray, C.B. Nonaqueous Synthesis of TiO_2 Nanocrystals Using TiF4 to Engineer Morphology, Oxygen Vacancy Concentration, and Photocatalytic Activity. *J. Am. Chem. Soc.* **2012**, *134*, 6751–6761. [CrossRef]
53. Liu, S.; Yu, J.; Jaroniec, M. Anatase TiO_2 with dominant high-energy {001} facets: Synthesis, properties, and applications. *Chem. Mater.* **2011**, *23*, 4085–4093. [CrossRef]
54. Brinker, C.J.; Scherer, G.W. *Sol-Gel Science: The Physics and Chemistry of Sol-Gel Processing*; Academic Press: Cambridge, MA, USA, 2013.
55. Sanchez, C.; Livage, J.; Henry, M.; Babonneau, F. Chemical modification of alkoxide precursors. *J. Non-Cryst. Solids* **1988**, *100*, 65–76. [CrossRef]
56. Gai, L.; Mei, Q.; Qin, X.; Li, W.; Jiang, H.; Duan, X. Controlled synthesis of anatase TiO_2 octahedra with enhanced photocatalytic activity. *Mater. Res. Bull.* **2013**, *48*, 4469–4475. [CrossRef]
57. Yu, J.; Liu, S.; Yu, H. Microstructures and photoactivity of mesoporous anatase hollow microspheres fabricated by fluoride-mediated self-transformation. *J. Catal.* **2007**, *249*, 59–66. [CrossRef]
58. Liao, J.; Luo, R.; Li, Y.B.; Zhang, J. Preparation of highly photocatalytically active rutile titania nanorods decorated with anatase nanoparticles produced by a titanyl-oxalato complex solution. *Mater. Sci. Semicond. Process.* **2013**, *16*, 2032–2038. [CrossRef]
59. Zhang, M.; Chen, T.; Wang, Y. Insights into TiO_2 polymorphs: Highly selective synthesis, phase transition, and their polymorph-dependent properties. *RSC Adv.* **2017**, *7*, 52755–52761. [CrossRef]
60. Zheng, Z.; Wang, Z.; Xie, L.; Fang, Z.; Feng, W.; Huang, M.; Liu, P. Synthesis of single-crystal-like TiO_2 hierarchical spheres with exposed {1 0 1} and {1 1 1} facets via lysine-inspired method. *Appl. Surf. Sci.* **2015**, *353*, 714–722. [CrossRef]
61. Möckel, H.; Giersig, M.; Willig, F. Formation of uniform size anatase nanocrystals from bis (ammonium lactato) titanium dihydroxide by thermohydrolysis. *J. Mater. Chem.* **1999**, *9*, 3051–3056. [CrossRef]
62. Seisenbaeva, G.A.; Daniel, G.; Nedelec, J.-M.; Kessler, V.G. Solution equilibrium behind the room-temperature synthesis of nanocrystalline titanium dioxide. *Nanoscale* **2013**, *5*, 3330–3336. [CrossRef]
63. Hernández-Gordillo, A.; Hernández-Arana, A.; Campero-Celis, A.; Vera-Robles, L.I. TiBALDH as a precursor for biomimetic TiO_2 synthesis: Stability aspects in aqueous media. *RSC Adv.* **2019**, *9*, 34559–34566. [CrossRef]
64. Hanprasopwattana, A.; Rieker, T.; Sault, A.G.; Datye, A.K. Morphology of titania coatings on silica gel. *Catal. Lett.* **1997**, *45*, 165–175. [CrossRef]
65. Hidalgo-Carrillo, J.; Martín-Gómez, J.; Herrera-Beurnio, M.C.; Estévez, R.C.; Urbano, F.J.; Marinas, A. Olive leaves as biotemplates for enhanced solar-light harvesting by a titania-based solid. *Nanomaterials* **2020**, *10*, 1057. [CrossRef]
66. Hashemizadeh, I.; Golovko, V.B.; Choi, J.; Tsang, D.C.; Yip, A.C. Photocatalytic reduction of CO_2 to hydrocarbons using bio-templated porous TiO_2 architectures under UV and visible light. *Chem. Eng. J.* **2018**, *347*, 64–73. [CrossRef]
67. Billet, J.; Dujardin, W.; De Keukeleere, K.; De Buysser, K.; De Roo, J.; Van Driessche, I. Size tunable synthesis and surface chemistry of metastable TiO_2-bronze nanocrystals. *Chem. Mater.* **2018**, *30*, 4298–4306. [CrossRef]
68. Truong, Q.D.; Le, T.H.; Hoa, H.T. Amino acid-assisted controlling the shapes of rutile, brookite for enhanced photocatalytic CO_2 reduction. *CrystEngComm* **2017**, *19*, 4519–4527. [CrossRef]
69. Ismail, A.A.; Kandiel, T.A.; Bahnemann, D.W. Novel (and better?) titania-based photocatalysts: Brookite nanorods and mesoporous structures. *J. Photochem. Photobiol. A Chem.* **2010**, *216*, 183–193. [CrossRef]
70. Hao, Y.; Rui, Y.; Li, Y.; Zhang, Q.; Wang, H. Size-tunable TiO_2 nanocrystals from titanium (IV) bis (ammonium lactato) dihydroxide and towards enhance the performance of dye-sensitized solar cells. *Electrochim. Acta* **2014**, *117*, 268–275. [CrossRef]
71. Tong, Z.; Yang, D.; Xiao, T.; Tian, Y.; Jiang, Z. Biomimetic fabrication of g-C_3N_4/TiO_2 nanosheets with enhanced photocatalytic activity toward organic pollutant degradation. *Chem. Eng. J.* **2015**, *260*, 117–125. [CrossRef]
72. Shi, J.; Yang, D.; Jiang, Z.; Jiang, Y.; Liang, Y.; Zhu, Y.; Wang, X.; Wang, H. Simultaneous size control and surface functionalization of titania nanoparticles through bioadhesion-assisted bio-inspired mineralization. *J. Nanoparticle Res.* **2012**, *14*, 1120. [CrossRef]
73. Cole, K.E.; Valentine, A.M. Spermidine and spermine catalyze the formation of nanostructured titanium oxide. *Biomacromolecules* **2007**, *8*, 1641–1647. [CrossRef] [PubMed]
74. Yan, Y.; Hao, B.; Wang, X.; Chen, G. Bio-inspired synthesis of titania with polyamine induced morphology and phase transformation at room-temperature: Insight into the role of the protonated amino group. *Dalton Trans.* **2013**, *42*, 12179–12184. [CrossRef]
75. Dickerson, M.B.; Jones, S.E.; Cai, Y.; Ahmad, G.; Naik, R.R.; Kröger, N.; Sandhage, K.H. Identification and design of peptides for the rapid, high-yield formation of nanoparticulate TiO2 from aqueous solutions at room temperature. *Chem. Mater.* **2008**, *20*, 1578–1584. [CrossRef]
76. Buckle, E.L.; Lum, J.S.; Roehrich, A.M.; Stote, R.E.; Vandermoon, B.; Dracinsky, M.; Filocamo, S.F.; Drobny, G.P. Serine–lysine peptides as mediators for the production of titanium dioxide: Investigating the effects of primary and secondary structures using solid-state NMR spectroscopy and DFT calculations. *J. Phys. Chem. B* **2018**, *122*, 4708–4718. [CrossRef]

77. Yang, G.; Guo, Q.; Kong, H.; Luan, X.; Wei, G. Structural design, biomimetic synthesis, and environmental sustainability of graphene-supported gC_3N_4/TiO_2 hetero-aerogels. *Environ. Sci. Nano* **2023**, *10*, 1257–1267. [CrossRef]
78. Sewell, S.L.; Wright, D.W. Biomimetic Synthesis of Titanium Dioxide Utilizing the R5 Peptide Derived from Cylindrotheca F Usiformis. *Chem. Mater.* **2006**, *18*, 3108–3113. [CrossRef]
79. Stote, R.E.; Filocamo, S.F.; Lum, J.S. Silaffin primary structure and its effects on the precipitation morphology of titanium dioxide. *J. Mater. Res.* **2016**, *31*, 1373–1382. [CrossRef]
80. Bregnhøj, M.; Lutz, H.; Roeters, S.J.; Lieberwirth, I.; Mertig, R.; Weidner, T. The diatom peptide R5 fabricates two-dimensional titanium dioxide nanosheets. *J. Phys. Chem. Lett.* **2022**, *13*, 5025–5029. [CrossRef] [PubMed]
81. Hellner, B.; Stegmann, A.E.; Pushpavanam, K.; Bailey, M.J.; Baneyx, F. Phase control of nanocrystalline inclusions in bioprecipitated titania with a panel of mutant silica-binding proteins. *Langmuir* **2020**, *36*, 8503–8510. [CrossRef]
82. Jiang, Y.; Yang, D.; Zhang, L.; Li, L.; Sun, Q.; Zhang, Y.; Li, J.; Jiang, Z. Biomimetic synthesis of titania nanoparticles induced by protamine. *Dalton Trans.* **2008**, 4165–4171. [CrossRef]
83. Gardères, J.; Elkhooly, T.A.; Link, T.; Markl, J.S.; Müller, W.E.; Renkel, J.; Korzhev, M.; Wiens, M. Self-assembly and photocatalytic activity of branched silicatein/silintaphin filaments decorated with silicatein-synthesized TiO_2 nanoparticles. *Bioprocess Biosyst. Eng.* **2016**, *39*, 1477–1486. [CrossRef]
84. Cheng, H.; Ma, J.; Zhao, Z.; Qi, L. Hydrothermal preparation of uniform nanosize rutile and anatase particles. *Chem. Mater.* **1995**, *7*, 663–671. [CrossRef]
85. Testino, A.; Bellobono, I.R.; Buscaglia, V.; Canevali, C.; D'Arienzo, M.; Polizzi, S.; Scotti, R.; Morazzoni, F. Optimizing the photocatalytic properties of hydrothermal TiO_2 by the control of phase composition and particle morphology. A systematic approach. *J. Am. Chem. Soc.* **2007**, *129*, 3564–3575. [CrossRef]
86. Shin, H.; Jung, H.S.; Hong, K.S.; Lee, J.-K. Crystallization process of TiO_2 nanoparticles in an acidic solution. *Chem. Lett.* **2004**, *33*, 1382–1383. [CrossRef]
87. Durupthy, O.; Bill, J.; Aldinger, F. Bioinspired synthesis of crystalline TiO_2: Effect of amino acids on nanoparticles structure and shape. *Cryst. Growth Des.* **2007**, *7*, 2696–2704. [CrossRef]
88. Zhang, G.; Zhang, T.; Li, B.; Zhang, X.; Chen, X. Biomimetic synthesis of interlaced mesh structures TiO_2 nanofibers with enhanced photocatalytic activity. *J. Alloys Compd.* **2016**, *668*, 113–120. [CrossRef]
89. Gautam, A.; Kshirsagar, A.; Biswas, R.; Banerjee, S.; Khanna, P.K. Photodegradation of organic dyes based on anatase and rutile TiO_2 nanoparticles. *RSC Adv.* **2016**, *6*, 2746–2759. [CrossRef]
90. He, Z.; Que, W.; He, Y. Synthesis and characterization of bioinspired hierarchical mesoporous TiO_2 photocatalysts. *Mater. Lett.* **2013**, *94*, 136–139. [CrossRef]
91. Hariharan, D.; Christy, A.J.; Mayandi, J.; Nehru, L. Visible light active photocatalyst: Hydrothermal green synthesized TiO_2 NPs for degradation of picric acid. *Mater. Lett.* **2018**, *222*, 45–49. [CrossRef]
92. Sundrarajan, M.; Bama, K.; Bhavani, M.; Jegatheeswaran, S.; Ambika, S.; Sangili, A.; Nithya, P.; Sumathi, R. Obtaining titanium dioxide nanoparticles with spherical shape and antimicrobial properties using M. citrifolia leaves extract by hydrothermal method. *J. Photochem. Photobiol. B Biol.* **2017**, *171*, 117–124.
93. Thandapani, K.; Kathiravan, M.; Namasivayam, E.; Padiksan, I.A.; Natesan, G.; Tiwari, M.; Giovanni, B.; Perumal, V. Enhanced larvicidal, antibacterial, and photocatalytic efficacy of TiO_2 nanohybrids green synthesized using the aqueous leaf extract of Parthenium hysterophorus. *Environ. Sci. Pollut. Res.* **2018**, *25*, 10328–10339. [CrossRef]
94. Balaji, S.; Guda, R.; Mandal, B.K.; Kasula, M.; Ubba, E.; Khan, F.-R.N. Green synthesis of nano-titania (TiO_2 NPs) utilizing aqueous Eucalyptus globulus leaf extract: Applications in the synthesis of 4 H-pyran derivatives. *Res. Chem. Intermed.* **2021**, *47*, 3919–3931. [CrossRef]
95. Zeebaree, A.Y.S.; Zeebaree, S.Y.S.; Rashid, R.F.; Zebari, O.I.H.; Albarwry, A.J.S.; Ali, A.F.; Zebari, A.Y.S. Sustainable engineering of plant-synthesized TiO_2 nanocatalysts: Diagnosis, properties and their photocatalytic performance in removing of methylene blue dye from effluent. A review. *Curr. Res. Green Sustain. Chem.* **2022**, *5*, 100312. [CrossRef]
96. Pushpavanam, K.; Hellner, B.; Baneyx, F. Interrogating biomineralization one amino acid at a time: Amplification of mutational effects in protein-aided titania morphogenesis through reaction-diffusion control. *Chem. Commun.* **2021**, *57*, 4803–4806. [CrossRef]
97. Katagiri, K.; Inami, H.; Ishikawa, T.; Koumoto, K. Enzyme-Assisted Synthesis of Titania under Ambient Conditions. *J. Am. Ceram. Soc.* **2009**, *92*, S181–S184. [CrossRef]
98. Nayak, J.; Meher, S.; Begum, G.; Seth, S.; Rana, R.K. Bioinspired Mineralization and Assembly Route to Integrate TiO_2 and Carbon Nitride Nanostructures: Designing Microstructures for Photoregeneration of NADH. *ACS Appl. Nano Mater.* **2023**, *6*, 13708–13719. [CrossRef]
99. Lu, Z.; Zhou, H.F.; Liao, J.J.; Yang, Y.Y.; Wang, K.; Che, L.M.; He, N.; Chen, X.D.; Song, R.; Cai, W.F.; et al. A facile dopamine-assisted method for the preparation of antibacterial surfaces based on Ag/TiO_2 nanoparticles. *Appl. Surf. Sci.* **2019**, *481*, 1270–1276. [CrossRef]
100. Hayami, Y.; Suzuki, Y.; Sagawa, T.; Yoshikawa, S. TiO_2 Rutile Nanorod Arrays Grown on FTO Substrate Using Amino Acid at a Low Temperature. *J. Nanosci. Nanotechnol.* **2010**, *10*, 2284–2291. [CrossRef]
101. Bakre, P.V.; Tilve, S.G.; Ghosh, N.N. Investigation of amino acids as templates for the sol–gel synthesis of mesoporous nano TiO_2 for photocatalysis. *Monatshefte Für Chem. -Chem. Mon.* **2018**, *149*, 11–18. [CrossRef]

102. Tao, Y.-G.; Xu, Y.-Q.; Pan, J.; Gu, H.; Qin, C.-Y.; Zhou, P. Glycine assisted synthesis of flower-like TiO_2 hierarchical spheres and its application in photocatalysis. *Mater. Sci. Eng. B* **2012**, *177*, 1664–1671. [CrossRef]
103. Ding, S.; Huang, F.; Mou, X.; Wu, J.; Lü, X. Mesoporous hollow TiO_2 microspheres with enhanced photoluminescence prepared by a smart amino acid template. *J. Mater. Chem.* **2011**, *21*, 4888–4892. [CrossRef]
104. Bakre, P.V.; Volvoikar, P.S.; Vernekar, A.A.; Tilve, S. Influence of acid chain length on the properties of TiO_2 prepared by sol-gel method and LC-MS studies of methylene blue photodegradation. *J. Colloid Interface Sci.* **2016**, *474*, 58–67. [CrossRef]
105. Guo, Y.; Lin, S.; Li, X.; Liu, Y. Amino acids assisted hydrothermal synthesis of hierarchically structured ZnO with enhanced photocatalytic activities. *Appl. Surf. Sci.* **2016**, *384*, 83–91. [CrossRef]
106. Lin, S.; Guo, Y.; Li, X.; Liu, Y. Glycine acid-assisted green hydrothermal synthesis and controlled growth of WO_3 nanowires. *Mater. Lett.* **2015**, *152*, 102–104. [CrossRef]
107. Wu, S.; Cao, H.; Yin, S.; Liu, X.; Zhang, X. Amino acid-assisted hydrothermal synthesis and photocatalysis of SnO_2 nanocrystals. *J. Phys. Chem. C* **2009**, *113*, 17893–17898. [CrossRef]
108. Jancik Prochazkova, A.; Demchyshyn, S.; Yumusak, C.; Masilko, J.; Bruggemann, O.; Weiter, M.; Kaltenbrunner, M.; Sariciftci, N.S.; Krajcovic, J.; Salinas, Y. Proteinogenic amino acid assisted preparation of highly luminescent hybrid perovskite nanoparticles. *ACS Appl. Nano Mater.* **2019**, *2*, 4267–4274. [CrossRef]
109. Kang, L.; Xu, P.; Chen, D.; Zhang, B.; Du, Y.; Han, X.; Li, Q.; Wang, H.-L. Amino acid-assisted synthesis of hierarchical silver microspheres for single particle surface-enhanced Raman spectroscopy. *J. Phys. Chem. C* **2013**, *117*, 10007–10012. [CrossRef]
110. Hong, C.-B.; Zhu, D.-J.; Ma, D.-D.; Wu, X.-T.; Zhu, Q.-L. An effective amino acid-assisted growth of ultrafine palladium nanocatalysts toward superior synergistic catalysis for hydrogen generation from formic acid. *Inorg. Chem. Front.* **2019**, *6*, 975–981. [CrossRef]
111. Duan, W.; Li, A.; Chen, Y.; Zhang, J.; Zhuo, K. Amino acid-assisted preparation of reduced graphene oxide-supported PtCo bimetallic nanospheres for electrocatalytic oxidation of methanol. *J. Appl. Electrochem.* **2019**, *49*, 413–421. [CrossRef]
112. Chen, Y.; Luo, X.; Luo, Y.; Xu, P.; He, J.; Jiang, L.; Li, J.; Yan, Z.; Wang, J. Efficient charge carrier separation in l-alanine acids derived N-TiO_2 nanospheres: The role of oxygen vacancies in tetrahedral Ti4+ sites. *Nanomaterials* **2019**, *9*, 698. [CrossRef]
113. Wu, X.; Liu, J.; Chen, Z.; Yang, Q.; Li, C.; Lu, G.; Wang, L. Amino acid assisted synthesis of mesoporous TiO_2 nanocrystals for high performance dye-sensitized solar cells. *J. Mater. Chem.* **2012**, *22*, 10438–10440. [CrossRef]
114. Liu, C.; Jiang, Z.; Tong, Z.; Li, Y.; Yang, D. Biomimetic synthesis of inorganic nanocomposites y a de novo designed peptide. *RSC Adv.* **2014**, *4*, 434–441. [CrossRef]
115. Kanie, K.; Sugimoto, T. Shape control of anatase TiO_2 nanoparticles by amino acids in a gel–sol system. *Chem. Commun.* **2004**, 1584–1585. [CrossRef]
116. Ayorinde, T.; Sayes, C.M. An updated review of industrially relevant titanium dioxide and its environmental health effects. *J. Hazard. Mater. Lett.* **2023**, *4*, 100085. [CrossRef]
117. Dolai, J.; Mandal, K.; Jana, N.R. Nanoparticle Size Effects in Biomedical Applications. *ACS Appl. Nano Mater.* **2021**, *4*, 6471–6496. [CrossRef]
118. Xie, Y.; Kocaefe, D.; Chen, C.; Kocaefe, Y. Review of Research on Template Methods in Preparation of Nanomaterials. *J. Nanomater.* **2016**, *2016*, 2302595. [CrossRef]
119. Ghaedi, H.; Zhao, M. Review on Template Removal Techniques for Synthesis of Mesoporous Silica Materials. *Energy Fuels* **2022**, *36*, 2424–2446. [CrossRef]
120. Tran, T.H.; Nosaka, A.Y.; Nosaka, Y. Adsorption and photocatalytic decomposition of amino acids in TiO_2 photocatalytic systems. *J. Phys. Chem. B* **2006**, *110*, 25525–25531. [CrossRef] [PubMed]
121. Fleming, G.J.; Adib, K.; Rodriguez, J.A.; Barteau, M.A.; White, J.M.; Idriss, H. The adsorption and reactions of the amino acid proline on rutile TiO_2(010) surfaces. *Surf. Sci.* **2008**, *602*, 2029–2038. [CrossRef]
122. Shchelokov, A.; Palko, N.; Potemkin, V.; Grishina, M.; Morozov, R.; Korina, E.; Uchaev, D.; Krivtsov, I.; Bol'shakov, O. Adsorption of Native Amino Acids on Nanocrystalline TiO_2: Physical Chemistry, QSPR, and Theoretical Modeling. *Langmuir* **2019**, *35*, 538–550. [CrossRef]
123. Pászti, Z.; Guczi, L. Amino acid adsorption on hydrophilic TiO_2: A sum frequency generation vibrational spectroscopy study. *Vib. Spectrosc.* **2009**, *50*, 48–56. [CrossRef]
124. Lee, N.; Sverjensky, D.A.; Hazen, R.M. Cooperative and Competitive Adsorption of Amino Acids with Ca^{2+} on Rutile (α-TiO_2). *Environ. Sci. Technol.* **2014**, *48*, 9358–9365. [CrossRef]
125. Brandt, E.G.; Lyubartsev, A.P. Molecular Dynamics Simulations of Adsorption of Amino Acid Side Chain Analogues and a Titanium Binding Peptide on the TiO_2 (100) Surface. *J. Phys. Chem. C* **2015**, *119*, 18126–18139. [CrossRef]
126. Ustunol, I.B.; Gonzalez-Pech, N.I.; Grassian, V.H. pH-dependent adsorption of α-amino acids, lysine, glutamic acid, serine and glycine, on TiO_2 nanoparticle surfaces. *J. Colloid Interface Sci.* **2019**, *554*, 362–375. [CrossRef]
127. Agosta, L.; Zollo, G.; Arcangeli, C.; Buonocore, F.; Gala, F.; Celino, M. Water driven adsorption of amino acids on the (101) anatase TiO_2 surface: An ab initio study. *Phys. Chem. Chem. Phys.* **2015**, *17*, 1556–1561. [CrossRef]
128. Xue, M.J.; Sampath, J.; Gebhart, R.N.; Haugen, H.J.; Lyngstadaas, S.P.; Pfaendtner, J.; Drobny, G. Studies of Dynamic Binding of Amino Acids to TiO_2 Nanoparticle Surfaces by Solution NMR and Molecular Dynamics Simulations. *Langmuir* **2020**, *36*, 10341–10350. [CrossRef] [PubMed]

129. Sampath, J.; Kullman, A.; Gebhart, R.; Drobny, G.; Pfaendtner, J. Molecular recognition and specificity of biomolecules to titanium dioxide from molecular dynamics simulations. *npj Comput. Mater.* **2020**, *6*, 34. [CrossRef]
130. Pantaleone, S.; Rimola, A.; Sodupe, M. Canonical, deprotonated, or zwitterionic? II. A computational study on amino acid interaction with the TiO_2(110) rutile surface: Comparison with the anatase (101) surface. *Phys. Chem. Chem. Phys.* **2020**, *22*, 16862–16876. [CrossRef]
131. Sano, K.-I.; Shiba, K. A hexapeptide motif that electrostatically binds to the surface of titanium. *J. Am. Chem. Soc.* **2003**, *125*, 14234–14235. [CrossRef] [PubMed]
132. Chang, Y.; Liu, X.; Cai, A.; Xing, S.; Ma, Z. Glycine-assisted synthesis of mesoporous TiO_2 nanostructures with improved photocatalytic activity. *Ceram. Int.* **2014**, *40*, 14765–14768. [CrossRef]
133. Senna, M.; Myers, N.; Aimable, A.; Laporte, V.; Pulgarin, C.; Baghriche, O.; Bowen, P. Modification of titania nanoparticles for photocatalytic antibacterial activity via a colloidal route with glycine and subsequent annealing. *J. Mater. Res.* **2013**, *28*, 354–361. [CrossRef]
134. Payan, A.; Fattahi, M.; Roozbehani, B. Synthesis, characterization and evaluations of TiO_2 nanostructures prepared from different titania precursors for photocatalytic degradation of 4-chlorophenol in aqueous solution. *J. Environ. Health Sci. Eng.* **2018**, *16*, 41–54. [CrossRef]
135. Jia, H.; Xiao, W.-J.; Zhang, L.; Zheng, Z.; Zhang, H.; Deng, F. In situ L-hydroxyproline functionalization and enhanced photocatalytic activity of TiO_2 nanorods. *J. Phys. Chem. C* **2008**, *112*, 11379–11384. [CrossRef]
136. Sarigul, G.; Chamorro-Mena, I.; Linares, N.; García-Martínez, J.; Serrano, E. Hybrid Amino Acid-TiO_2 Materials with Tuneable Crystalline Structure and Morphology for Photocatalytic Applications. *Adv. Sustain. Syst.* **2021**, *5*, 2100076. [CrossRef]
137. Goutam, S.P.; Saxena, G.; Singh, V.; Yadav, A.K.; Bharagava, R.N.; Thapa, K.B. Green synthesis of TiO_2 nanoparticles using leaf extract of Jatropha curcas L. for photocatalytic degradation of tannery wastewater. *Chem. Eng. J.* **2018**, *336*, 386–396. [CrossRef]
138. Leng, J.; Zhao, Y.; Zhang, J.; Bai, X.; Zhang, A.; Li, Q.; Huang, M.; Wang, J. Synthesis of In-Modified TiO_2 Composite Materials from Waste Tobacco Stem Silk and Study of Their Catalytic Performance under Visible Light. *Catalysts* **2024**, *14*, 615. [CrossRef]
139. Zangeneh, H.; Mousavi, S.A.; Eskandari, P. Comparison the visible photocatalytic activity and kinetic performance of amino acids (non-metal doped) TiO_2 for degradation of colored wastewater effluent. *Mater. Sci. Semicond. Process.* **2022**, *140*, 106383. [CrossRef]
140. Zangeneh, H.; Mousavi, S.A.; Eskandari, P.; Amarloo, E.; Farghelitiyan, J.; Mohammadi, S. Comparative Study on Photocatalytic Performance of TiO_2 Doped with Different Amino Acids in Degradation of Antibiotics. *Water* **2023**, *15*, 535. [CrossRef]
141. Zhou, H.; Ding, L.; Fan, T.; Ding, J.; Zhang, D.; Guo, Q. Leaf-inspired hierarchical porous CdS/Au/N-TiO_2 heterostructures for visible light photocatalytic hydrogen evolution. *Appl. Catal. B Environ.* **2014**, *147*, 221–228. [CrossRef]
142. Mallakpour, S.; Aalizadeh, R. A simple and convenient method for the surface coating of TiO_2 nanoparticles with bioactive chiral diacids containing different amino acids as the coupling agent. *Prog. Org. Coat.* **2013**, *76*, 648–653. [CrossRef]
143. Stavert, T.; Patwardhan, S.V.; Pilling, R.; Jorge, M. Unlocking the holy grail of sustainable and scalable mesoporous silica using computational modelling. *RSC Sustain.* **2023**, *1*, 432–438. [CrossRef]
144. Dewulf, L.; Chiacchia, M.; Yeardley, A.S.; Milton, R.A.; Brown, S.F.; Patwardhan, S.V. Designing bioinspired green nanosilicas using statistical and machine learning approaches. *Mol. Syst. Des. Eng.* **2021**, *6*, 293–307. [CrossRef]
145. Williamson, E.M.; Sun, Z.; Mora-Tamez, L.; Brutchey, R.L. Design of Experiments for Nanocrystal Syntheses: A How-To Guide for Proper Implementation. *Chem. Mater.* **2022**, *34*, 9823–9835. [CrossRef]
146. Norfolk, L.; Dewulf, L.; Chiacchia, M.; Patwardhan, S.V.; Staniland, S.S. Simultaneous optimisation of shape and magnetisation of nanoparticles synthesised using a green bioinspired route. *Mol. Syst. Des. Eng.* **2024**, *9*, 300–310. [CrossRef]
147. Coley, C.W.; Green, W.H.; Jensen, K.F. Machine learning in computer-aided synthesis planning. *Acc. Chem. Res.* **2018**, *51*, 1281–1289. [CrossRef]
148. Tao, H.; Wu, T.; Aldeghi, M.; Wu, T.C.; Aspuru-Guzik, A.; Kumacheva, E. Nanoparticle synthesis assisted by machine learning. *Nat. Rev. Mater.* **2021**, *6*, 701–716. [CrossRef]
149. Katoueizadeh, E.; Zebarjad, S.M.; Janghorban, K. Optimization of synthesis conditions of N-doped TiO_2 nanoparticles using Taguchi robust design. *Mater. Chem. Phys.* **2017**, *201*, 69–77. [CrossRef]
150. Sun, L.; An, T.; Wan, S.; Li, G.; Bao, N.; Hu, X.; Fu, J.; Sheng, G. Effect of synthesis conditions on photocatalytic activities of nanoparticulate TiO_2 thin films. *Sep. Purif. Technol.* **2009**, *68*, 83–89. [CrossRef]
151. Gao, B.; Sun, M.; Ding, Z.; Liu, W. Machine learning-optimized synthesis of doped TiO_2 with improved photocatalytic performance: A multi-step workflow supported by designed wet-lab experiments. *J. Alloys Compd.* **2021**, *881*, 160534. [CrossRef]
152. Pellegrino, F.; Isopescu, R.; Pellutiè, L.; Sordello, F.; Rossi, A.M.; Ortel, E.; Martra, G.; Hodoroaba, V.-D.; Maurino, V. Machine learning approach for elucidating and predicting the role of synthesis parameters on the shape and size of TiO_2 nanoparticles. *Sci. Rep.* **2020**, *10*, 18910. [CrossRef]
153. DeVierno Kreuder, A.; House-Knight, T.; Whitford, J.; Ponnusamy, E.; Miller, P.; Jesse, N.; Rodenborn, R.; Sayag, S.; Gebel, M.; Aped, I.; et al. A Method for Assessing Greener Alternatives between Chemical Products Following the 12 Principles of Green Chemistry. *ACS Sustain. Chem. Eng.* **2017**, *5*, 2927–2935. [CrossRef]
154. Brambila, C.; Boyd, P.; Keegan, A.; Sharma, P.; Vetter, C.; Ponnusamy, E.; Patwardhan, S.V. A Comparison of Environmental Impact of Various Silicas Using a Green Chemistry Evaluator. *ACS Sustain. Chem. Eng.* **2022**, *10*, 5288–5298. [CrossRef]

155. Patwardhan, S.V.; Staniland, S.S. Case study 2: Silica. In *Green Nanomaterials: From Bioinspired Synthesis to Sustainable Manufacturing of Inorganic Nanomaterials*; IOP Publishing: Bristol, UK, 2019; ISBN 978-0-7503-1221-9.
156. Jundale, R.B.; Sonawane, J.R.; Palghadmal, A.V.; Jaiswal, H.K.; Deore, H.S.; Kulkarni, A.A. Scaling-up continuous production of mesoporous silica particles at kg scale: Design & operational strategies. *React. Chem. Eng.* **2024**, *9*, 1914–1923. [CrossRef]
157. Baba, Y.D.; Chiacchia, M.; Patwardhan, S.V. A Novel Method for Understanding the Mixing Mechanisms to Enable Sustainable Manufacturing of Bioinspired Silica. *ACS Eng. Au* **2023**, *3*, 17–27. [CrossRef]
158. Pilling, R.; Patwardhan, S.V. Recent Advances in Enabling Green Manufacture of Functional Nanomaterials: A Case Study of Bioinspired Silica. *ACS Sustain. Chem. Eng.* **2022**, *10*, 12048–12064. [CrossRef]
159. Drummond, C.; McCann, R.; Patwardhan, S.V. A feasibility study of the biologically inspired green manufacturing of precipitated silica. *Chem. Eng. J.* **2014**, *244*, 483–492. [CrossRef]
160. Yan, M.; Martell, S.; Dasog, M.; Brown, S.; Patwardhan, S.V. Cost-competitive manufacture of porous-silicon anodes via the magnesiothermic reduction: A techno-economic analysis. *J. Power Sources* **2023**, *588*, 233720. [CrossRef]
161. Ashworth, D.J.; Driver, J.; Sasitharan, K.; Prasad, R.R.R.; Nicks, J.; Smith, B.J.; Patwardhan, S.V.; Foster, J.A. Scalable and sustainable manufacturing of ultrathin metal–organic framework nanosheets (MONs) for solar cell applications. *Chem. Eng. J.* **2023**, *477*, 146871. [CrossRef]
162. Pottier, A.; Chaneac, C.; Tronc, E.; Mazerolles, L.; Jolivet, J.P. Synthesis of brookite TiO_2 nanoparticles by thermolysis of $TiCl_4$ in strongly acidic aqueous media. *J. Mater. Chem.* **2001**, *11*, 1116–1121. [CrossRef]
163. Chen, K.-Y.; Chen, Y.-W. Synthesis of spherical titanium dioxide particles by homogeneous precipitation in acetone solution. *J. Sol-Gel Sci. Technol.* **2003**, *27*, 111–117. [CrossRef]
164. Zhou, Y.; Antonietti, M. Synthesis of very small TiO_2 nanocrystals in a room-temperature ionic liquid and their self-assembly toward mesoporous spherical aggregates. *J. Am. Chem. Soc.* **2003**, *125*, 14960–14961. [CrossRef]
165. Boppella, R.; Basak, P.; Manorama, S.V. Viable Method for the Synthesis of Biphasic TiO_2 Nanocrystals with Tunable Phase Composition and Enabled Visible-Light Photocatalytic Performance. *ACS Appl. Mater. Interfaces* **2012**, *4*, 1239–1246. [CrossRef]
166. Yasin, A.; Guo, F.; Demopoulos, G.P. Continuous-reactor, pH-controlled synthesis of multifunctional mesoporous nanocrystalline anatase aggregates. *Chem. Eng. J.* **2016**, *287*, 398–409. [CrossRef]
167. Gopal, M.; Chan, W.M.; De Jonghe, L. Room temperature synthesis of crystalline metal oxides. *J. Mater. Sci.* **1997**, *32*, 6001–6008. [CrossRef]
168. Chemseddine, A.; Moritz, T. Nanostructuring titania: Control over nanocrystal structure, size, shape, and organization. *Eur. J. Inorg. Chem.* **1999**, *1999*, 235–245. [CrossRef]
169. Nadzirah, S.; Foo, K.; Hashim, U. Morphological reaction on the different stabilizers of titanium dioxide nanoparticles. *Int. J. Electrochem. Sci.* **2015**, *10*, 5498–5512. [CrossRef]
170. Patra, S.; Davoisne, C.; Bruyère, S.; Bouyanfif, H.; Cassaignon, S.; Taberna, P.L.; Sauvage, F. Room-Temperature Synthesis of High Surface Area Anatase TiO_2 Exhibiting a Complete Lithium Insertion Solid Solution. *Part. Part. Syst. Charact.* **2013**, *30*, 1093–1104. [CrossRef]
171. Gao, Y.; Wang, H.; Wu, J.; Zhao, R.; Lu, Y.; Xin, B. Controlled facile synthesis and photocatalytic activity of ultrafine high crystallinity TiO_2 nanocrystals with tunable anatase/rutile ratios. *Appl. Surf. Sci.* **2014**, *294*, 36–41. [CrossRef]
172. Fischer, K.; Grimm, M.; Meyers, J.; Dietrich, C.; Gläser, R.; Schulze, A. Photoactive microfiltration membranes via directed synthesis of TiO_2 nanoparticles on the polymer surface for removal of drugs from water. *J. Membr. Sci.* **2015**, *478*, 49–57. [CrossRef]
173. Ahmed, M.; Abou-Gamra, Z.; Medien, H.; Hamza, M. Effect of porphyrin on photocatalytic activity of TiO_2 nanoparticles toward Rhodamine B photodegradation. *J. Photochem. Photobiol. B Biol.* **2017**, *176*, 25–35. [CrossRef]
174. Wang, L.; Wu, D.; Guo, Z.; Yan, J.; Hu, Y.; Chang, Z.; Yuan, Q.; Ming, H.; Wang, J. Ultra-thin TiO_2 sheets with rich surface disorders for enhanced photocatalytic performance under simulated sunlight. *J. Alloys Compd.* **2018**, *745*, 26–32. [CrossRef]
175. Wu, Z.; Xue, Y.; Zou, Z.; Wang, X.; Gao, F. Single-crystalline titanium dioxide hollow tetragonal nanocones with large exposed (1 0 1) facets for excellent photocatalysis. *J. Colloid Interface Sci.* **2017**, *490*, 420–429. [CrossRef]